Thermal gradient effects on Uranium - 10% w/o molybdenum alloys

Avallone, Eugene Michael; Bosnak, Robert J.

Massachusetts Institute of Technology

THERMAL GRADIENT EFFECTS ON URANIUM - 10%w/o MOLYBDENUM ALLOYS

EUGENE MICHAEL AVALLONE
and
ROBERT JOHN BOSNAK

THERMAL GRADIENT EFFECTS ON URANIUM - 10% w/o MOLYBDENUM ALLOYS

by

Eugene Michael Avallone
B. S., United States Naval Academy
(1952)

and

Robert John Bosnak
B. S., United States Coast Guard Academy
(1948)

Submitted in Partial Fulfillment of the
Requirements for the Degree of NAVAL ENGINEER

and

for the Degree of MASTER OF SCIENCE in
Naval Architecture and Marine Engineering

at the

MASSACHUSETTS INSTITUTE OF TECHNOLOGY

MAY, 1960

THERMAL GRADIENT EFFECTS ON URANIUM - 10% w/o MOLYBDENUM ALLOYS

by

Eugene Michael Avallone

and

Robert John Bosnak

Submitted to the Department of Naval Architecture and Marine Engineering on May 21, 1960, in partial fulfillment of the requirements for the Master of Science Degree in Naval Architecture and Marine Engineering and for the Professional Degree, Naval Engineer.

ABSTRACT

This thesis has as its general objective the evaluation of the effects of a thermal gradient on a Uranium-10% w/o molybdenum alloy. This fuel alloy will be used in the Enrico Fermi Fast Breeder Reactor and is being considered for other reactors. A U-10% w/o Mo alloy contains enough Mo to stabilize the isotropic gamma phase at room temperatures. However previous work on its transformation kinetics indicate that when at elevated temperatures for sufficient time, the gamma phase transforms to the undesirable, anisotropic alpha plus delta phases. These are undesirable for use in a reactor because of dimensional instability.

The experiments conducted imposed on this alloy temperature gradients comparative to those in an operating reactor. The purpose was to find what the effects of such gradients would be on the transformation kinetics of the alloy, and on the movements of molybdenum and carbon within the alloy.

These effects were measured by means of X-ray diffraction, micro-hardness, metallographic inspection, electron microbeam probe analysis, and chemical analysis. It was found by these methods that the transformation zone (from gamma to alpha plus delta) begins in the alloy at a time sooner than two hours and continues to grow in size for the longer time runs. There was no significant carbon or molybdenum diffusion detected.

On this basis the Fermi Reactor fuel pins will transform after a relatively short period of operation. However the effects of radiation on this transformation are not yet thoroughly understood. Earlier work indicates radiation may act to retard or inhibit transformation. It is recommended that further experimental work be conducted at longer times, and if possible at steeper gradients, to determine whether or not carbon and molybdenum diffusion can be detected. The next logical step would be to repeat this work in a radiation field to determine its effect.

Thesis Supervisor: Robert E. Ogilvie

Title: Assistant Professor of Metallurgy

ACKNOWLEDGEMENTS

The authors would like to acknowledge their indebtedness to those who have assisted in the preparation of this thesis: To Nuclear Metals, Inc., for the use of their facilities; to Engelhard Industries, D. E. Makepeace Division for the provision of the fuel alloy used; to the M.I.T. Metallurgy Department for the generous loan of equipment.

In particular we wish to express our thanks and gratitude to the following:

At M. I. T.	Professor R. E. Ogilvie Mr. Robert Huston Mr. Tom Flanagan
At Nuclear Metals, Inc.	Dr. Albert R. Kaufmann Mr. Joseph E. Roman Mr. John M. Siergiej Miss Harriet P. Roth Miss Gladys G. Kay Mr. Ernest J. Bonnafe Mr. Stanley H. Gelles
At Engelhard Industries D.E. Makepeace Div.	Mr. Richard Saglio

The authors especially wish to express their sincere appreciation to Professor Robert E. Ogilvie of the Department of Metallurgy at M.I.T. who acted as thesis supervisor.

TABLE OF CONTENTS

LISTING OF TEXT TABLES

LISTING OF APPENDIX TABLES

LIST OF FIGURES AND ILLUSTRATIONS

List of Figures and Illustrations Continued....

I. INTRODUCTION AND STATEMENT OF PROBLEM

Unalloyed uranium normally exists in three phases: alpha, an orthorhombic structure to 663°C; beta, a tetragonal structure from 663°C to 770°C; and gamma, a body centered cubic structure from 770°C to the melting point at 1133°C. Alpha uranium is highly anisotropic as may be evidenced from Table I-1.

TABLE I-1

Irradiation and Thermal Growth Coefficients for Alpha Uranium

Direction	Irradiation Growth Coefficient 10^{-6} ppm Burnup	Thermal Expansion Coefficient 10^{-6} per °C
(100)	-420 ± 20	21.7
(010)	$+420 \pm 20$	- 1.5
(001)	0 ± 20	23.2

On irradiation, as on thermal cycling, a severe dimensional change takes place in alpha uranium. These changes vary with direction which complicates the problem. In view of these difficulties, uranium in its stable state (alpha) at room temperature is not particularly useful for reactor use. Gamma uranium on the other hand behaves isotropically on irradiation or thermal cycling, and therefore would be better suited for service in a reactor. The use of gamma uranium presents one

serious problem and that is it is not a stable state at room temperatures. A great deal of research has been done in the last decade on attempting to alloy uranium with various metals in order to stabilize the gamma phase at room temperatures. With such an alloy, uranium could then be used in a reactor without fear of encountering the anisotropic properties of alpha uranium.

Molybdenum, zirconium, or niobium when added to uranium in sufficient quantities form alloys with uranium which stabilize the gamma phase at room temperature. In addition, these metals tend to increase the corrosion resistance of uranium. It would seem that adding one of these elements to uranium would then solve the problem of anisotropy. This is true, but the gamma phase below 770°C is not a stable state for uranium. Thus the gamma phase formed by alloying is a metastable supersaturated solid solution state at room temperatures, which under certain conditions may transform to its natural or stable state, alpha uranium. With the alloying metal present the stable state at room temperature is alpha uranium plus a delta phase. The composition of the delta phase depends upon the transformation temperature.

Molybdenum has been used for the alloying element in several new reactor systems. Figures 1 and 2[10] show the fact that a 10% w/o Mo alloy will be stable at room temperatures if cooled from the gamma field within 20 hours. This rate of cooling, as shown in Fig. 2, is rapid enough to avoid encountering the transformation region and will

form a metastable supersaturated solid solution below the equilibrium range. As the molybdenum content is lowered to 6% or 7% w/o Mo, a much faster quench (approximately one hour) is needed to stabilize the gamma phase at room temperature.

Transformation kinetics for this system as shown in Fig. 2 are the work of the Armour Research Foundation and indicate that the temperature rate is a maximum in the region between 450°C and 500°C when cooling from the gamma phase takes place in a time greater than 20 hours.

It should be mentioned here that it has previously been noted[1, 4] that the amount of initial cold work and the amount of initial impurities present tends to have serious effect on the position of the nose of the TTT diagram. Increasing both tends to shift it to the left.

Early research on the 10% w/o Mo alloy[10] indicates that irradiation of the alloy will increase its stability below the equilibrium range. It has also been reported[21] that irradiation of the alpha plus delta phase will transform it to the metastable gamma phase. There has been no recent work reported in this area. What is needed is work on this alloy under the actual operating conditions it will face in a reactor where a steep temperature gradient and the intense radiation flux of neutrons, gamma rays, and fission fragments is present.

The first phase in such an undertaking would be to design and build the equipment and to run the necessary experiments without the radiation present. Then, after this has been completed, the second

phase would involve the same or similar experiments in a radiation flux.

This investigation has encompassed only the first phase just described and its objectives have been: (1) to ascertain what the effects of such a severe temperature gradient are on the transformation kinetics of the material; (2) to note whether or not any significant diffusion of the molybdenum takes place which would serve to deplete the fuel alloy to the extent where the normal transition of the uranium from gamma to the alpha plus delta phases would occur at an increased rate; (3) and finally to note the effect of the temperature gradient on the impurity, carbon, in the alloy to ascertain whether or not diffusion has occurred, and if so its possible effect on the transformation kinetics and the fuel alloy in general.

The alloy tested was a U-10% w/o Mo which is the identical material which will be used in the Enrico Fermi Fast Breeder Reactor where the maximum centerline uranium temperature is reported[10] as 612°C, with an outer surface uranium temperature at this point of 500°C. The fuel pin diameter is 0.158" including cladding (or 0.148" of bare U-Mo alloy), giving a gradient of approximately 1500°C per inch. The equipment used in the experimental work produced a maximum gradient of 1900°C per inch.

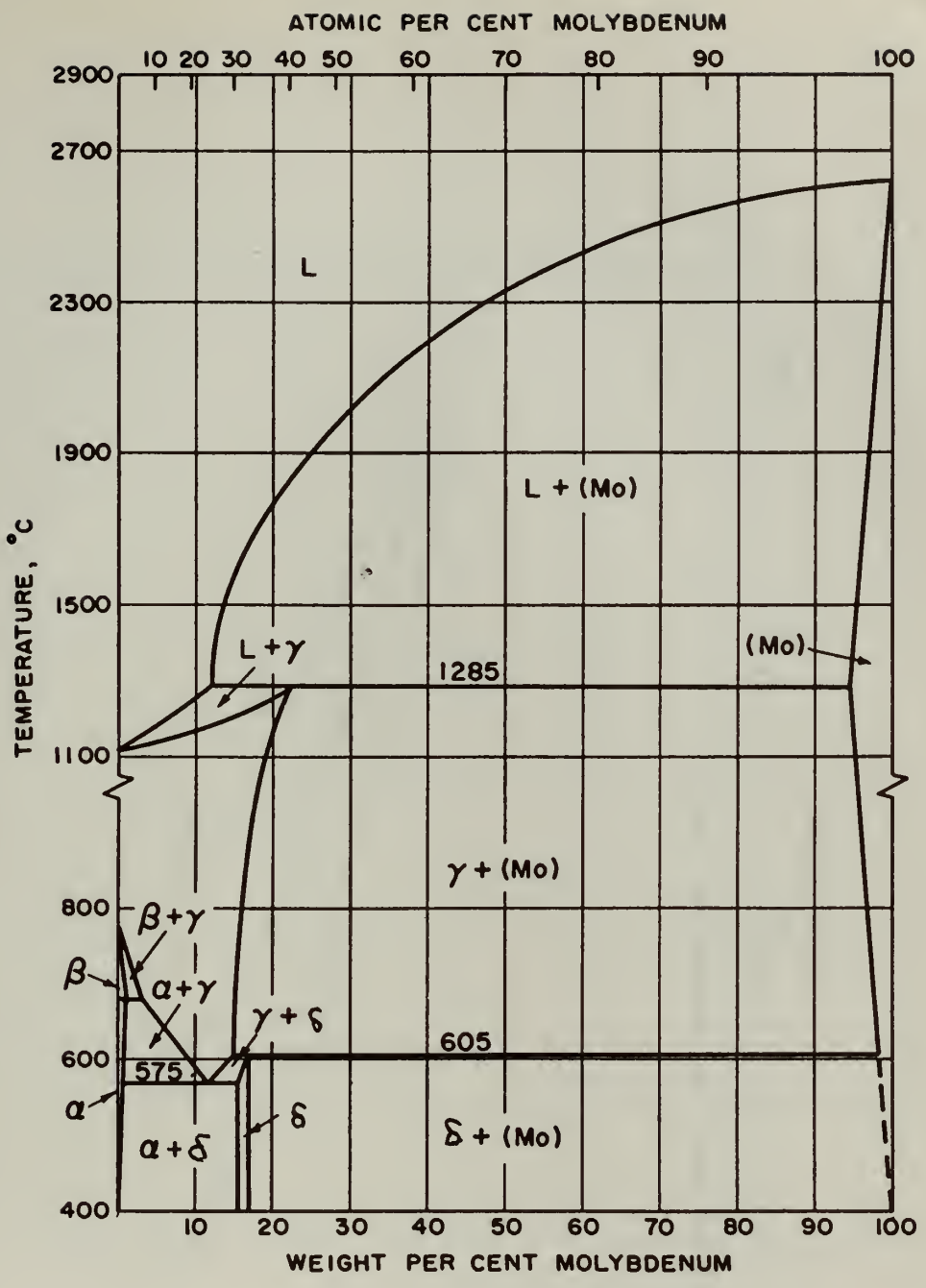

FIG. 1 URANIUM-MOLYBDENUM PHASE DIAGRAM

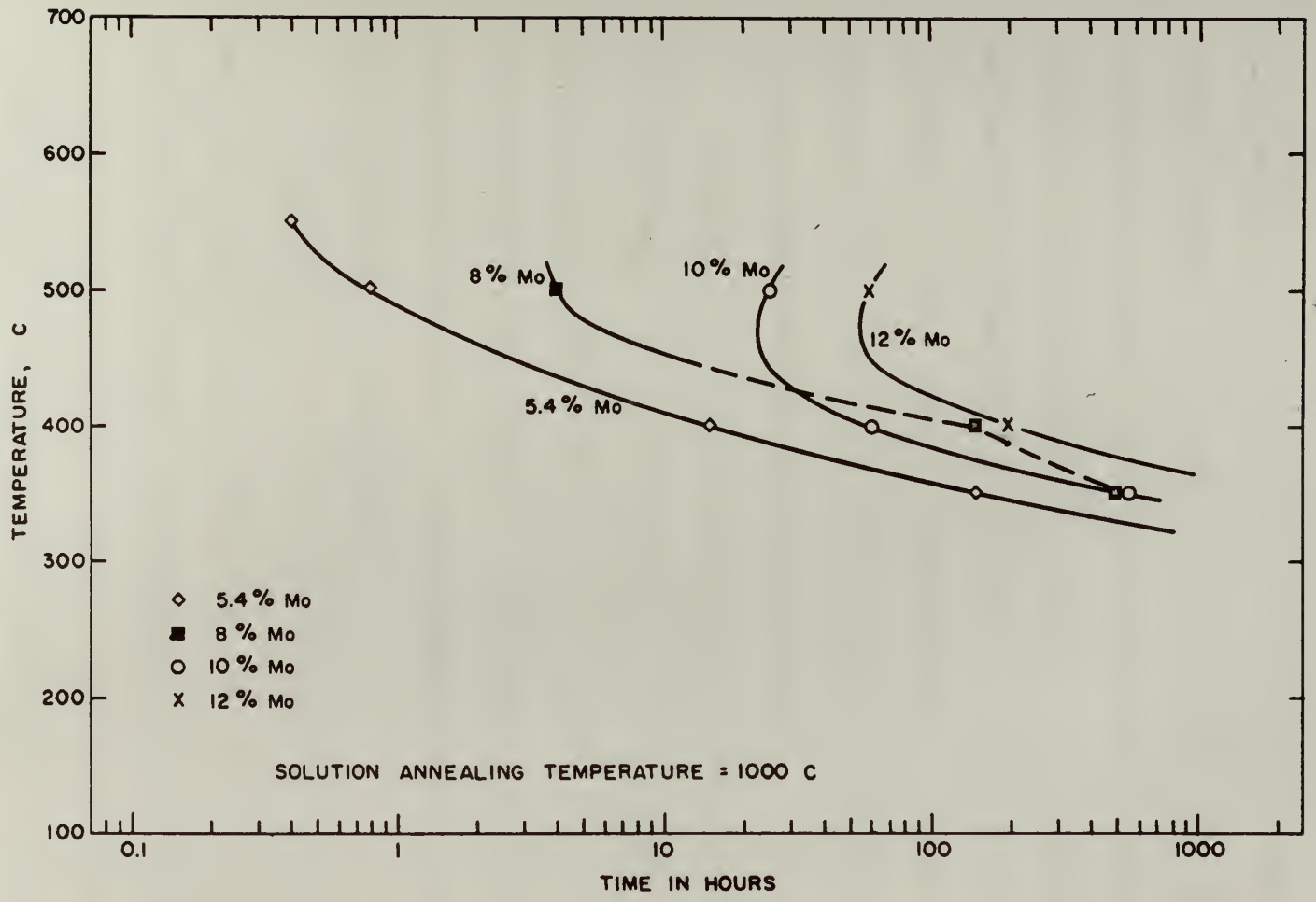

FIG. 2 TIME, TEMPERATURE, TRANSITION DIAGRAM FOR URANIUM-MOLYBDENUM ALLOYS

II. PRELIMINARY INVESTIGATION OF EQUIPMENT AND FINAL DESIGN

Since the effect of severe temperature gradients was to be investigated, a search was made of the literature pertaining to thermal diffusion furnaces. This study revealed that little work has been done in this area in the United States, while an equally thorough search of European literature disclosed that some work on non-radioactive metals has been done in Germany.[5] In all cases the system was not required to be evacuated thereby greatly simplifying experimental techniques and equipment design. Since in this case uranium would be operating at elevated temperatures, a vacuum was mandatory.

In settling on a design of the equipment actually used, many different configurations were considered. A conventional-type furnace was discarded because of difficulties in evacuation and in maintaining the desired temperature gradient. A new and novel approach to the problem was decided upon. Figure 3 shows the pyrex gradient furnace set-up as used in the experiments.

It was felt that the use of an all pyrex cross for the furnace enclosure would offer many advantages. First and foremost it would ease evacuation problems, it would provide good accessibility to the specimen, it would allow easy visual inspection of the sample, and it was relatively inexpensive. The measurement of the temperature gradient while maintaining a vacuum was the most difficult problem in the design. Several different approaches suggested themselves,

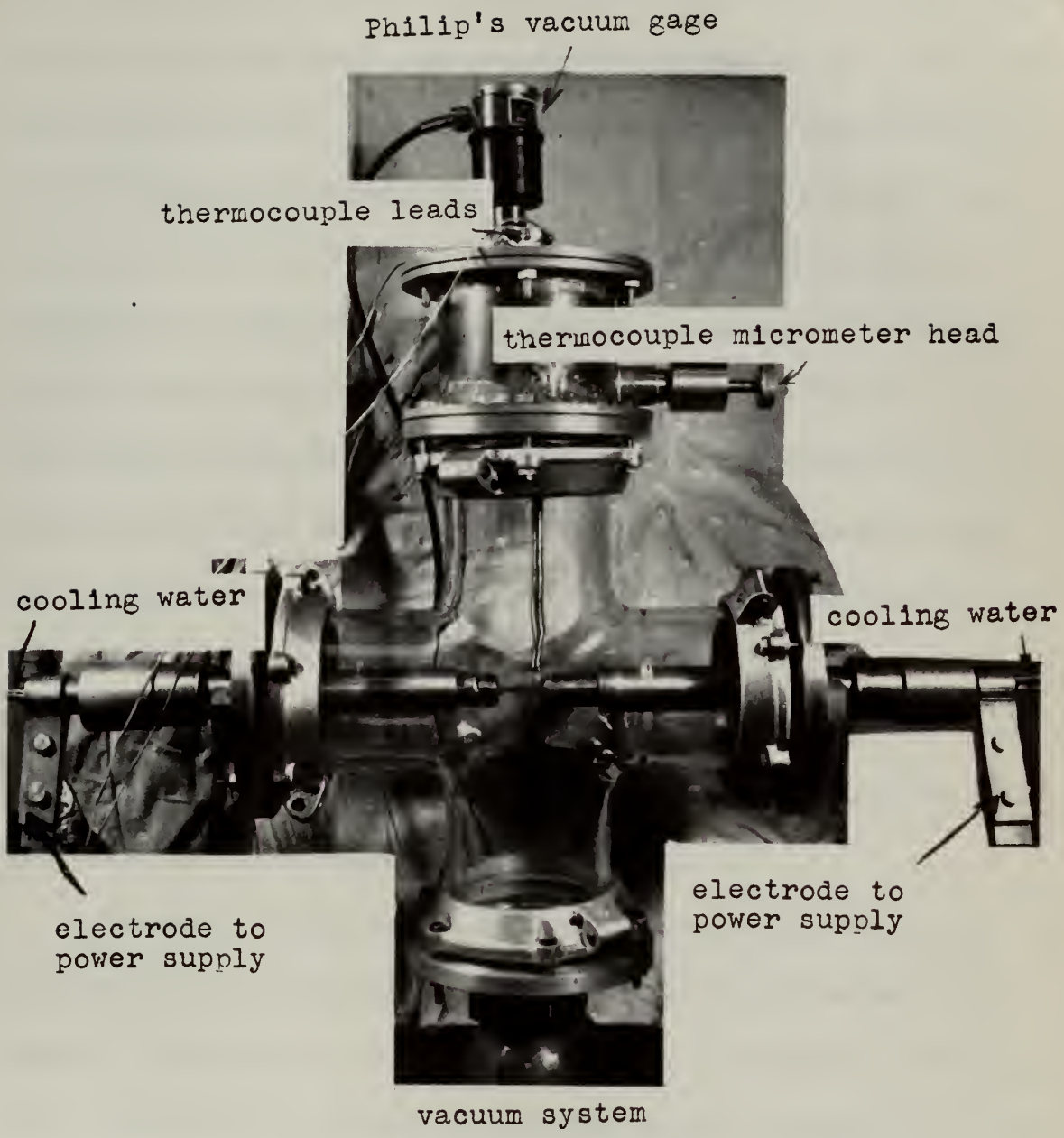

Figure 3 EQUIPMENT ARRANGEMENT

but it seemed there would be no ideal method. With each scheme some compromises would have to be accepted and in some cases severe design difficulties overcome. The method which immediately suggested itself for temperature measurement was an axially drilled hole through which the thermocouple could travel. This method was rejected since it presented very difficult problems involving the passage of the thermocouple system through the water cooled electrodes while still maintaining the required vacuum. Another method to measure the gradient, which had the advantage of giving both the temperature and its location on the sample, would have been to weld thermocouple junctions at fixed points on each specimen. This arrangement would entail bringing many such thermocouple leads through the vacuum seal, would make the changing of samples more difficult, and would not provide a continuous temperature measurement.

The method finally selected to measure the gradient was via a thermocouple which travels continuously across the top surface of the sample. Movement is accomplished by turning a threaded rod (40 threads per inch) which in turn pushes a sliding block which supports the thermocouple. The vacuum lead through for the thermocouple wires is via a glass to metal seal in the upper flange. With this arrangement a continuous measurement can be made of the surface temperature of the specimen (see Fig. 4). The method used to obtain the temperature along the specimen's axis is described in Section III-C and IV-C.

The next problem was attaining the gradient itself. The only method considered practical was resistance heating of the sample with water cooling of the electrodes in which the sample is held. By this method it was hoped to achieve a gradient of approximately 1800°C to 2000°C in one inch. (Refer to Fig. 5 for a detailed drawing of the water cooled electrodes.) Water flows from the source via a non-conducting tubing such as rubber or plastic to the entry tubing of the electrode which is at its center. The water flow is directed against a plate which served to reverse the water flow and also physically holds the sample and hence acts as a heat sink. The water flow back out of the hollow electrode is in the annulus formed by the inlet tube and the outer wall of the electrode. Finally connection to a drain is again made via non-conducting tubing. Flow of electricity (in this case AC) is via a strap fixed to the hollow electrode, through the specimen, and then out via the other electrode.

The specimen when at temperature may be considered essentially stress free since the electrodes are free to expand in the direction of the axis of the sample.

Since it was not desired to further complicate the results with the effects that might be caused if the heating source were direct current, an ordinaly AC welding transformer was selected as the current source. Since there was no external voltage regulation, it was recognized that fluctuations in line voltage would probably create fluctuations in current to the specimen of up to 3% or 4% which could possibly effect temperatures $\pm$ 25°C.

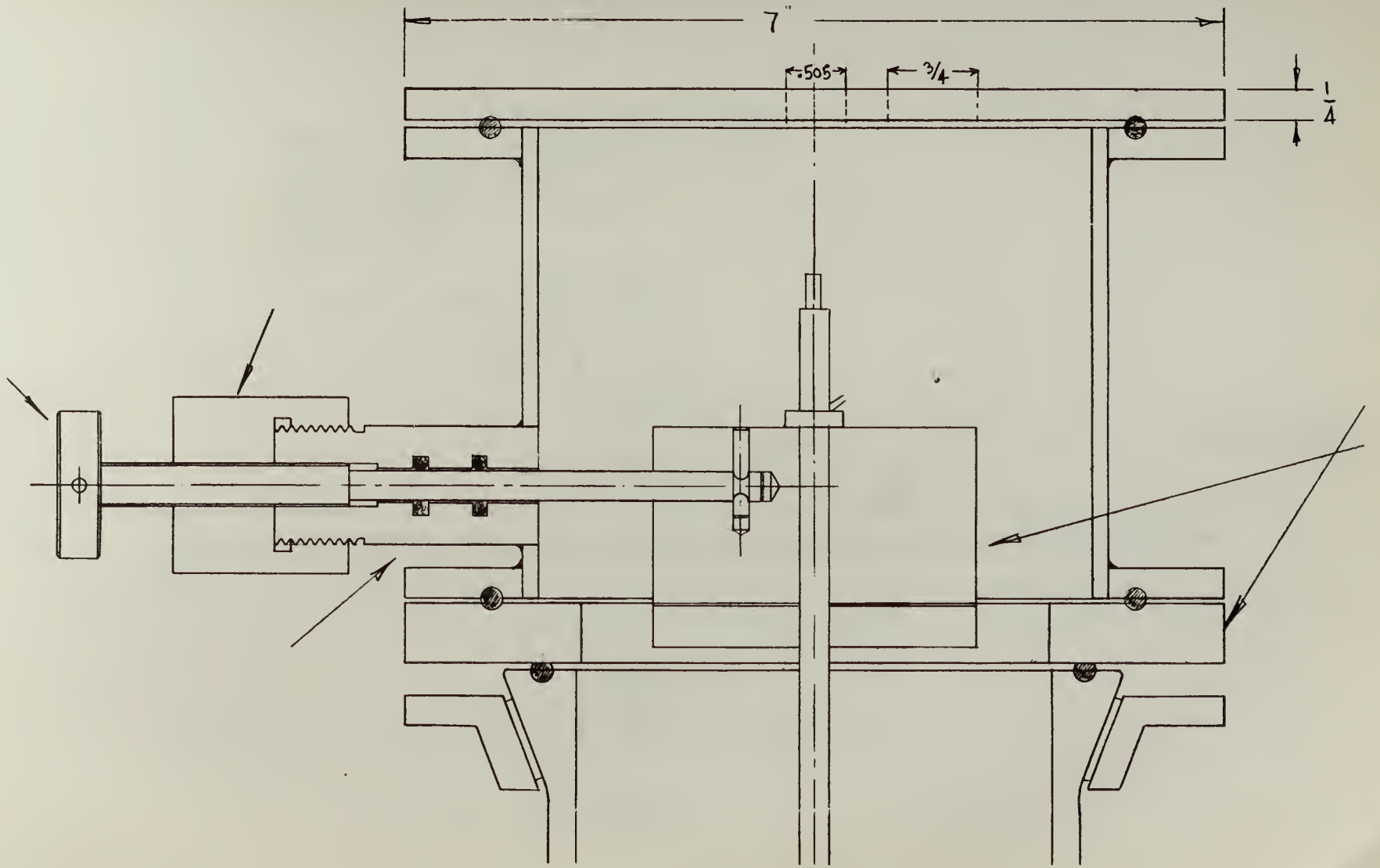

FIGURE 4 THERMOCOUPLE ASSEMBLY DRAWING

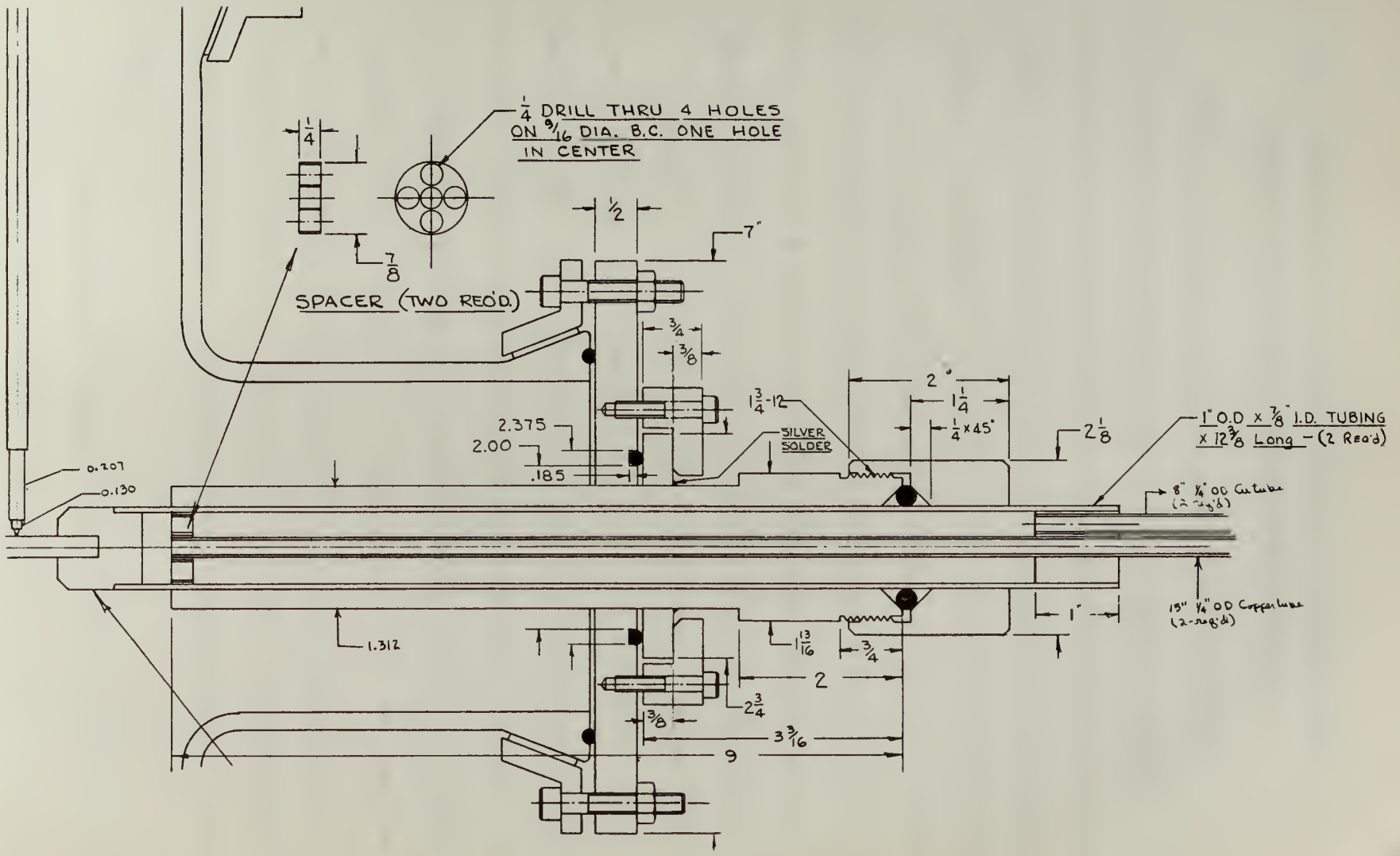

FIGURE 5 WATER-COOLED ELECTRODE ASSEMBLY DRAWING

III-A. PRELIMINARY WORK ON VACUUM, SPECIMEN SIZE, CURRENT SOURCE AND POWER REQUIREMENTS

With the equipment design completed and the furnace built, the next problem was to determine what vacuum could be obtained, and whether desired specimen temperatures could be reached. A standard roughing and diffusion pump set up (Cenco Megavac Vacuum Pump) gave vacuums of the order of 0.1 microns. This was considered adequate.

An AC welding transformer with a 57 ampere primary at 220 volts, and a 200 ampere 60 percent capacity secondary (P and H AC Arc Welder) was obtained for a power source. On trial runs, with a 0.25 inch outer diameter specimen of two inches in length, temperatures of 500°C could not be reached with the power supply. Two iron specimens which were tapered from 0.25 inch outer diameter ends to a 0.1250 inch outer diameter center section were tested. The specimens were 2 inches long with the 0.125 inch outer diameter section one inch in length. Using 161.6 amperes, temperatures of approximately 1000°C were reached in the center section. With higher currents one of the iron specimens was melted. Thus with the installed power supply, and specimens of an outer diameter of 0.125 inches, temperatures of 1000°C were attainable. Voltage measurements of the various samples ranged from 0.5 to 0.8 volts.

The next step was to determine what size O.D. would best suit the desired operating condition of approximately 1000°C at the center

A = 2.5"
B = 1.0"
C = 0.250"
D = 0.135"

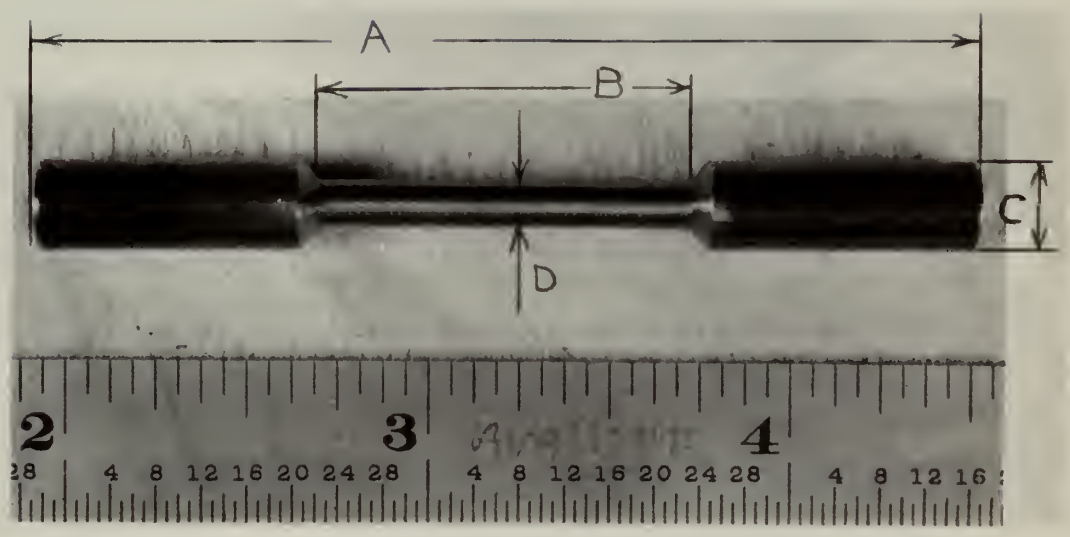

Figure 6 TYPICAL SPECIMEN USED IN RUNS

of our sample with temperatures as low as possible at the ends of the specimen. In order to preserve as much metal as possible for any required destructive testing of the specimen, the largest possible outer diameter was desirable. It was decided to test a series of samples of varying sizes in an attempt to determine the best size for our purposes.

Six test pieces were tried, all were two inches in length with 0.25 inch outer diameter at the ends. The center section of the specimens were varied as follows:

Length of Center Section	O.D. of Center Section
3/4 inches	0.160
1 inch	0.160
3/4 inches	0.135
1 inch	0.135
3/4 inches	0.125
1 inch	0.125

These test specimens were run at various currents and for various time periods.

Temperature profiles were taken on some of the runs to determine what temperatures were reached in the center, and how steep a gradient had been obtained. Upon completion of the test runs the 0.135 inch

outer diameter center section of one inch in length was chosen. The overall specimen size was increased to two and a half inches (2.5") to allow a longer section to fit into the water cooled electrodes (see Fig. 6). It was hoped that this would increase the heat transfer axially, and increase the gradient. The increased resistance resulted in the use of lower currents to attain the desired temperatures.

III-B. SAMPLE HISTORY

The material used for the specimens was generously furnished by Nuclear Metals, Inc., and the D. E. Makepeace Division of Engelhard Industries. The alloy material used consisted of depleted uranium and 10% molybdenum having a known impurity content of 1275 ppm Zr, 170 ppm carbon, 127 ppm iron and 137 ppm nickel. The working history included: the initial ingot melt at 1375°C; a homogenization heat treatment at 1075°C for 24 hours to insure the uniform distribution of the molybdenum; two extrusions at 1600°F, the latter one a coextrusion which clad the core with zirconium; cold swaging via 4 dies and approximately 6 passes per die from 0.325" to 0.250" diameter; two annealing passes, one after going through two dies to soften the material for further swaging, and the final pass after all swaging was complete to relieve internal stresses and soften the material, (both passes for 30 minutes at 1200°F); machining the center portion of the 0.250" specimen to the size shown in Fig. 6, and cutting to length to meet the needs of the equipment for resistance heating.

III-C. ACTUAL EXPERIMENTAL RUNS

Having selected a specimen of two and a half inches in length with an outer diameter of 0.25 inches at the ends, and a one inch long 0.135" outer diameter center section as the sample size, experimental runs were begun. A short run of four hours was made at first to determine what effects a thermal gradient would have on the fuel pin specimen. While this specimen was being prepared for analysis, a two hour run was also made.

Analysis of the four hour sample by microbeam probe showed that no molybdenum diffusion had occurred. Visual inspection of the specimen showed some changes in the surface at the junction of the 0.135 inch outer diameter section to the 0.25 inch outer diameter section. This is the region of the steepest thermal gradient (approximately 1900°C per inch). At this point it was decided to neglect the two hour specimen temporarily, and make a long run in order to attempt to bracket a region of interest. A run of one hundred hours duration was decided upon. If molybdenum diffusion could be detected, then shorter time runs could be made to determine when the diffusion actually begins. Also of interest was a determination of what phenomenon had been observed in the four hour specimen. While the hundred hour run was being made various etchants were tried on the four hour specimen.

Upon completion of the hundred hour run, another microbeam probe was conducted which showed that no molybdenum diffusion had occurred.

Metallographic analysis of the four hour and hundred hour runs were conducted. After polishing and etching visual inspection at 100 × showed that something had occurred in the region of the specimen's shoulder - that is where the 0.135 inch outer diameter section meets the 0.25 outer diameter section. This region on the specimen appeared to be a eutectoid region. To confirm this suspicion it was decided to make an X-ray diffraction study, and take some back deflection Laues of the region of interest.

While conducting the analysis of the four and hundred hour samples, another longtime run was being made to determine whether molybdenum diffusion might also be detected. This run was conducted for three hundred and fifteen hours. Once again, microbeam probe of the sample showed that no molybdenum diffusion had occurred. Metallographic analysis showed that this specimen also had a eutectoid type region at the shoulder.

The results of the X-ray diffraction and back deflection Laues of the shoulder region disclosed that the metastable gamma phase had transformed to the stable alpha plus delta eutectoid. This transformation occurred on the four hour run as well as the hundred hour and three hundred and fifteen hour runs. It was noted that the transformed region grew in width with the longer time runs. Therefore, the width of the transformed region should be time dependent. In order to gain more data to more accurately determine this relationship intermediate length runs were required.

Two more experimental runs were conducted. The first of ten hours duration, and the second of fifty hours. These two specimens and the two hour specimen were polished and etched. Examination of the eutectoid region at 100× and 500× were conducted and the region widths determined. As suspected the eutectoid region widths increase with longer length runs. Due to the nature of a eutectoid these regions should be harder. Microhardness readings were taken using a TUKON Microhardness Tester with a 136 degree diamond. The hardness data confirmed the visual observations. The region of hardness increased with the length of time for the runs.

The results of all this work are shown in the following section of the thesis:

	Section
Actual Experiments	IV-A
X-Ray Studies	IV-B
Hardness Curves	IV-C
Metallographic	IV-D
Diffusion	IV-E

The temperature profiles obtained for the runs are plotted with the hardness curves in section IV - C. A 50 percent Nitric Acid, 50 percent Sulphuric Acid and 5 percent Hydrofluoric Acid etch was used in every case except the three hundred and fifteen hour run. An electrolytic etch was used in that case to compare the effects of polarized light on the samples. With the acid etch all sections acted like cubic structure,

and reflected polarized light. In comparing this with the electrolytic etch, and the results of the X-ray diffraction and back deflection Laues it was shown that the oxide film resulting from the acid etch was causing the polarization effects in the transformed regions. This polarization effect was not noted in the transformed region when an electrolytic etch was used.

One final experimental run was conducted to determine what temperature difference existed between the surface and center of the specimen. Holes were drilled in a specimen along its length. The thermocouple was first placed adjacent to each hole on the surface of the specimen, and then dropped into the hole to get the temperature at the center of the specimen. The results are shown plotted with the hardness curves in section IV - C. No radiation shields were used during any of these runs. As shown on the curves of section IV - C, the surface to centerline temperature difference was greatest in the region where the specimen was hottest. This difference is undoubtedly due to radiation losses from the specimen's surface.

IV-A. ACTUAL EXPERIMENTS

For all the experimental runs the current and voltage was as follows:

Current	175.2 ± 22.8 amperes
Voltage	0.628 ± 0.15 volts

The numbers following the plus and minus signs are standard deviations. The temperature profiles for the runs are plotted with the hardness curves in section IV - C.

TABLE IV-1

Experimental Results Summary

Length of Run Hours	Gamma Transformation Occurred	Molybdenum Diffused	Width of Transformed Region in m.m.
2	Yes	No	1.91
4	Yes	No	2.29
10	Yes	No	2.66
50	Yes	No	3.01
100	Yes	No	3.39
315	Yes	No	4.64

IV-B. X-RAY STUDIES

Referring to the phase diagram of the U-Mo system (see Fig. 1), it is noted that for a 10% w/o Mo alloy below 575° one would expect the $\gamma \longrightarrow \alpha + \delta$ phase transformation if the transformation kinetics as shown in Fig. 2 permitted it. The delta (δ) phase has been studied by many investigators and it is generally agreed that it is an ordered body centered tetragonal structure. There has been a considerable amount of work taking place on the values of the delta phase lattic constants. Pfeil and Brown[7] report a = 3.425 Å and c = 3.282 Å. Tucker[3] reports the same and also reports the diffraction pattern based on this structure (tabulated in appendix). Saller and Halteman proposed in 1954 constants of a = 6.84 Å and c = 6.55 Å. A paper by R. J. VanThyne and D. J. McPherson published in 1957 showing X-ray diffractometer patterns used the above values of Saller and Halteman. A recent detailed analysis by Halteman[8, 11] leads to a = 3.427 and c = 9.834.

Table App.-IV-1 in the appendix lists the "d" values and h, k, l values as reported by Tucker[3] based on his "a" and "c" values. Obviously the observed "d" values will not change, and only the h, k, l directions will differ as the "a" and "c" values are modified.

The distance d_{hkl} between adjacent lattice planes in the uranium alloy involved in this study is best expressed by:

Orthorhombic Alpha

$$\frac{1}{d^2} = \left(\frac{h}{a}\right)^2 + \left(\frac{k}{b}\right)^2 + \left(\frac{l}{c}\right)^2 \qquad (1)$$

Tetragonal Delta

$$\frac{1}{d^2} = \frac{h^2 + k^2}{a^2} + \frac{l^2}{c^2} \qquad (2)$$

Cubic Gamma

$$\frac{1}{d^2} = \frac{h^2 + k^2 + l^2}{a^2} \qquad (3)$$

Using equation (2) above it is seen that the h, k, l values for each d value of Saller and Halteman will be double the k, k, l values of each corresponding d value reported by Tucker. For the latest work by Halteman, the Tucker h, k, l values would be h, k, 3l, respectively, for each d value tabulated.

Table App.-IV-1 in the appendix lists Tucker's observed "d" values, his h, k, l values and also the new Halteman h, k, l values.

Since the Halteman values appear to be the best and latest information, they will be used throughout this section and the appendix for work dealing with the delta phase.

A method suitable for determining if any phase transformations have taken place is via X-ray diffraction studies.

Bragg's law pertaining to the diffraction of X-rays from a crystal may be stated as:

$$\lambda = 2d \sin \theta \qquad (4)$$

where n is an integer (taken as = 1), λ is the wave length of the radiation used. In all cases for this work copper radiation with a nickel K_B filter is utilized so λ = 1.54 Å (the CuK_α X-ray), d is the spacing between atomic planes in the crystal, θ is the angle of incidence between the X-ray beam and the atomic plane.

Two different methods were used, both depending on Bragg's law. These were the back deflection Laue and an X-ray diffractometer. In the former the set up is as sketched in Fig. 7. The equations which apply are Bragg's law and from Fig. 7.

$$\text{Tan } \alpha = \frac{X}{3} \tag{5}$$

$$\alpha = 180° - 2\theta \tag{6}$$

$$\theta = \frac{180 - \alpha}{2} \tag{7}$$

$$d = \frac{\lambda}{2 \sin \theta} = \frac{0.77}{\sin \theta} \tag{8}$$

Where X is the radius of the circle observed on the plate in centimeters. Three (3) cm is the distance from photographic plate to specimen.

By the use of equations (5, 7, and 8) and the measurement of the radius of the Laue circles (see Figs. 9 to 12) the "d" values can be obtained. The complete data on the control and the 100 hour samples appears in the appendix Tables App.-IV-3 and App.-IV-4. The results of this study are summarized in Table IV-2.

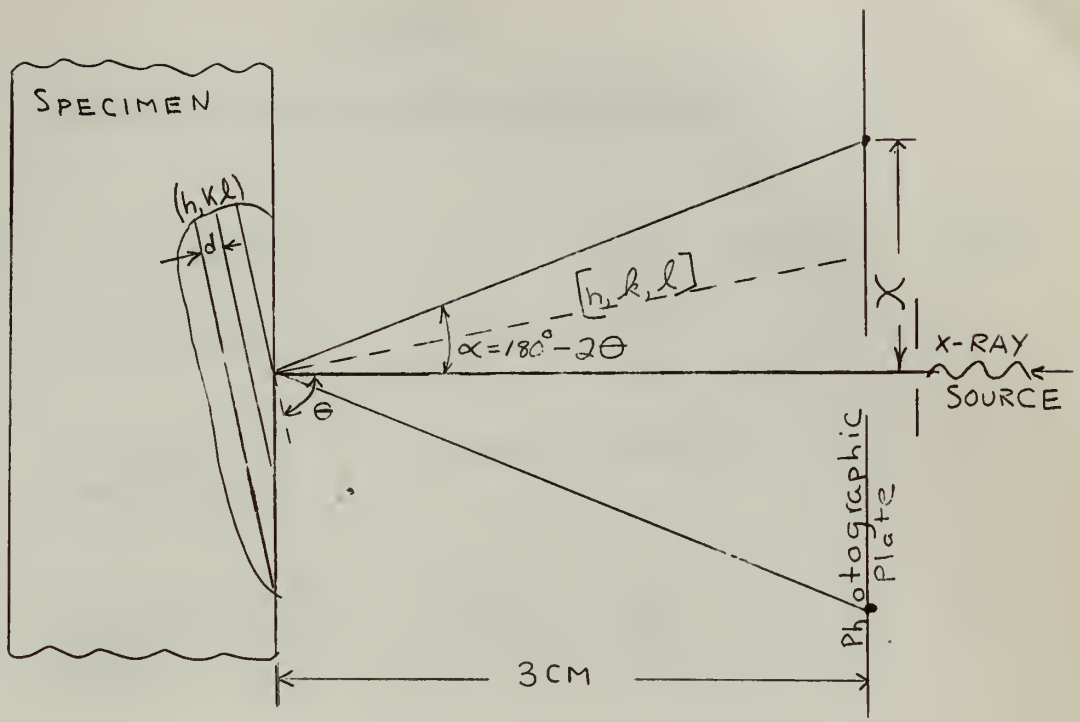

Figure 7. Back Deflection Laues

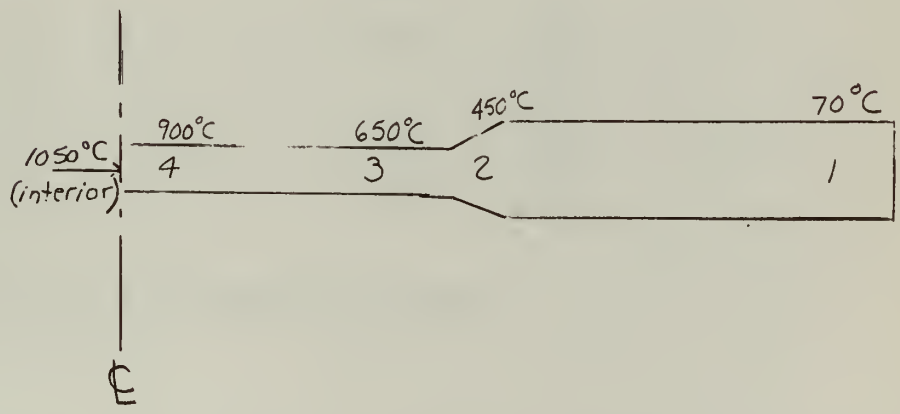

Figure 8. Cross Section of Specimen Showing Regions Used in X-Ray and Metallographic Studies, and an Approximate Surface Temperature which is Typical of the Region.

TABLE IV-2

Summary of Laue Results for 100 Hour Sample

Region*	Description	d Value	h,k,l	Material	Refer to Figure
1	Cold end untransformed	0.8046	411	γ	9
		0.8546	400	γ	
		0.9130	321	γ	
3	Warm end untransformed	Same as for region 1.			10
4	Hot region, large grains, untransformed	0.8046	411	γ	11
		0.8546	400	γ	
2	Transformation zone	0.805	411γ	γ or δ	12
			413δ		
		0.8154	313	α	
			154		
		0.843	135	α	
			331		
			063		
		0.855	400	γ or δ	
		0.892	129	δ	

* Refer to Fig. 8 for location on sample.

The control sample data over all its length is exactly the same as for region No. 1 of the 100 hour sample tabulated above (see Fig. 9).

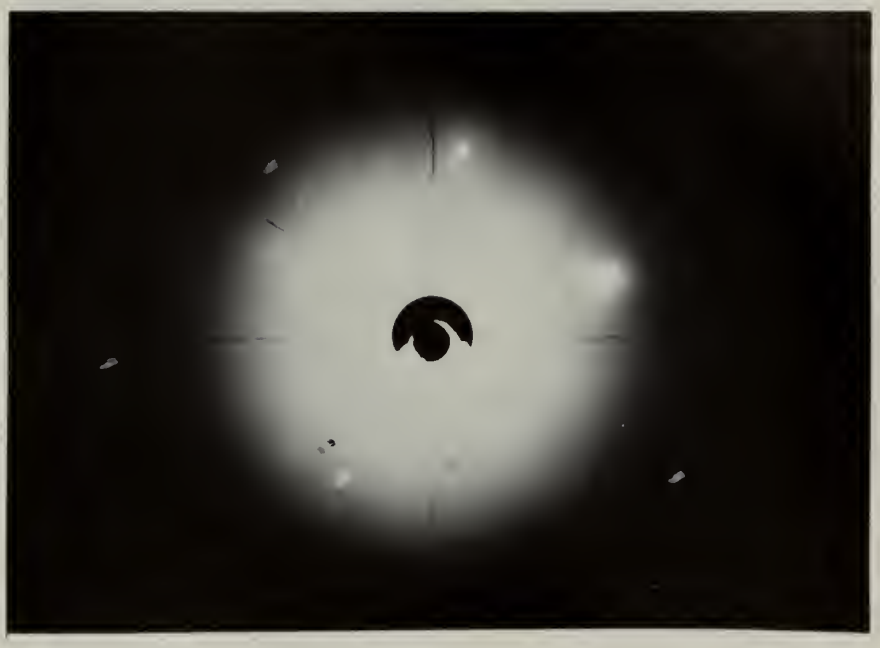

Figure 9 Back Deflection Laue, Control(all regions) and 100 Hour Sample(region1)

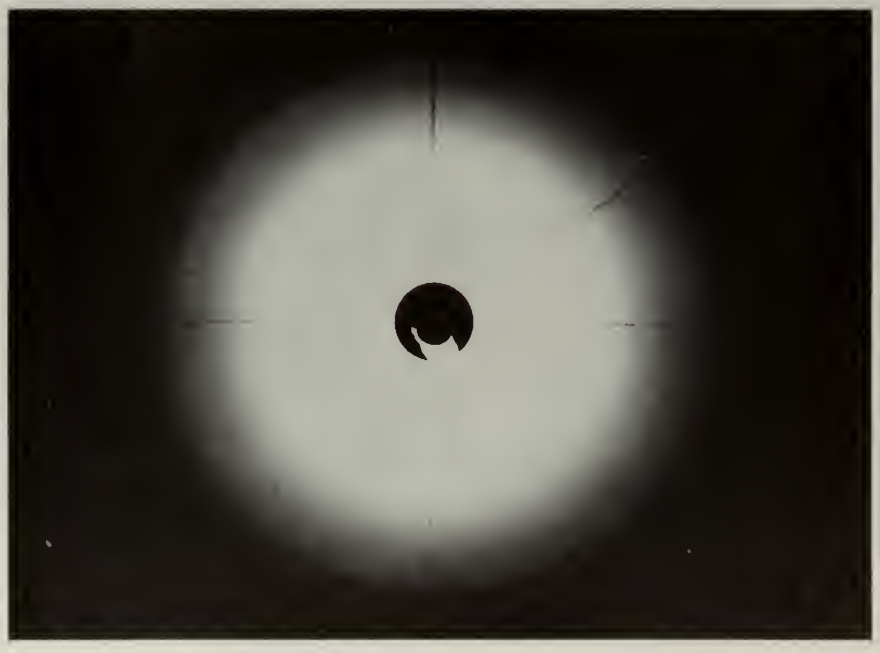

Figure 10 Back Deflection Laue, 100 Hour Sample (region 3)

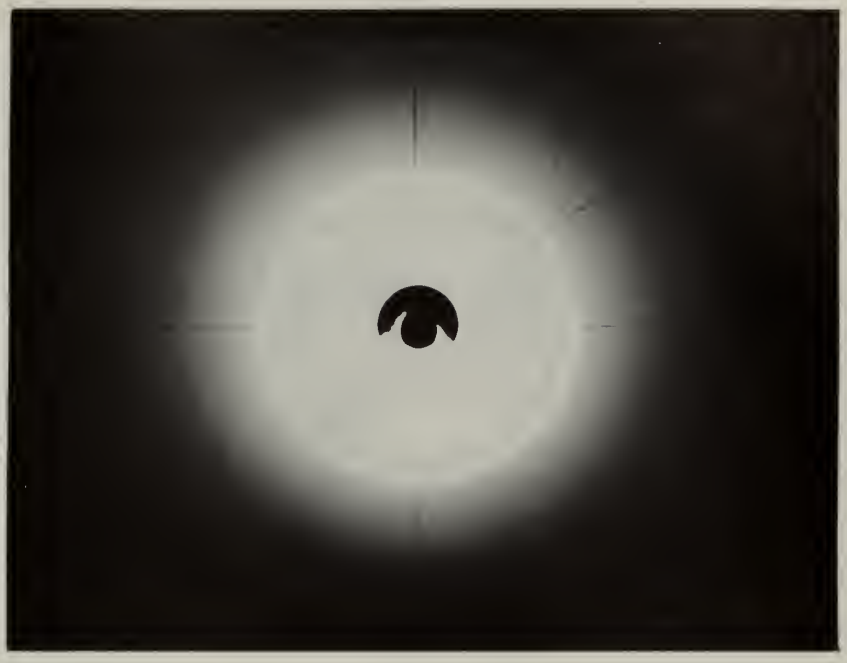

Figure 11 Back Deflection Laue, 100 Hour Sample (region 4)

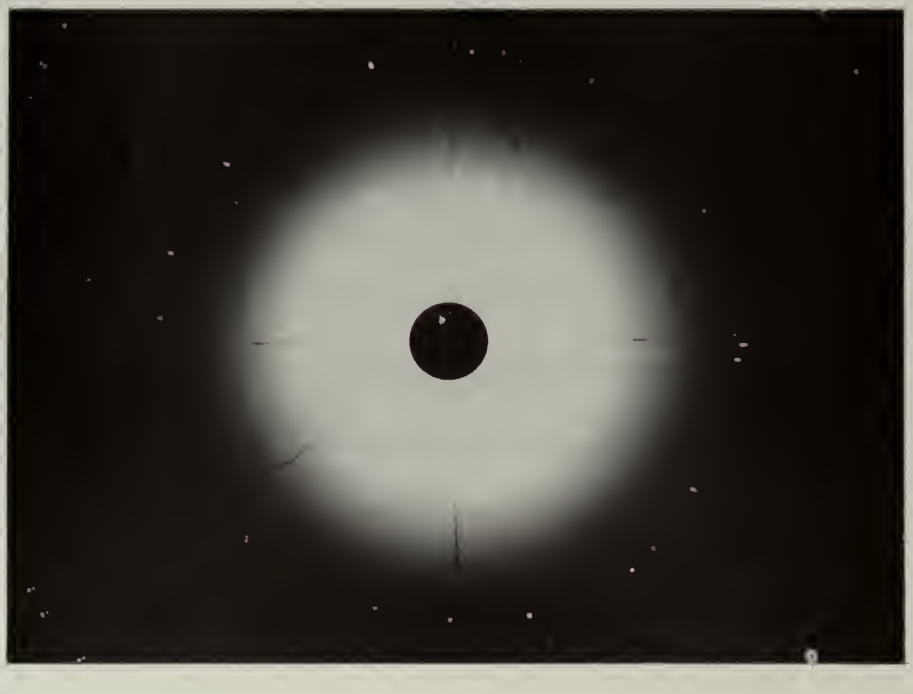

Figure 12 Back Deflection Laue, 100 Hour Sample (region 2)

The results then clearly indicate that in a band on the sample whose temperature is approximately 500°C (see Fig. 8) the gamma has transformed to alpha plus delta. Tables App.-IV-1 and App.-IV-2 in the appendix were used as "standards" to identify the alpha and delta phases.

X-Ray Diffractometer

Runs were made on a General Electric XRD3 diffractometer using Copper K_{α} radiation with a nickel K_{β} filter. The control, 100 hour, and 315 hour samples were the only ones treated. The latter two appeared to have sufficient $\alpha + \delta$ transformation regions to show up on the diffractometer easily.

Figure 13 represents a typical section of diffractometer pattern of the control or all gamma specimen showing the (110) peak. Figure 14 is the exact same section of the pattern for the 315 hour sample. Note that on Fig. 14, in addition to the (110) γ peak, d = 2.42, there also appears the peaks shown listed in Table IV-3. Figure 15 represents a section of the pattern of the control sample showing the (200) peak. Figure 16 is the exact same section for the 315 hour sample. Note that on Fig. 16 in addition to the (200)γ peak, d = 1.717, there also appears the peaks shown listed in Table IV-4. Figures 14 and 16 have a calibration correction of +0.5°.

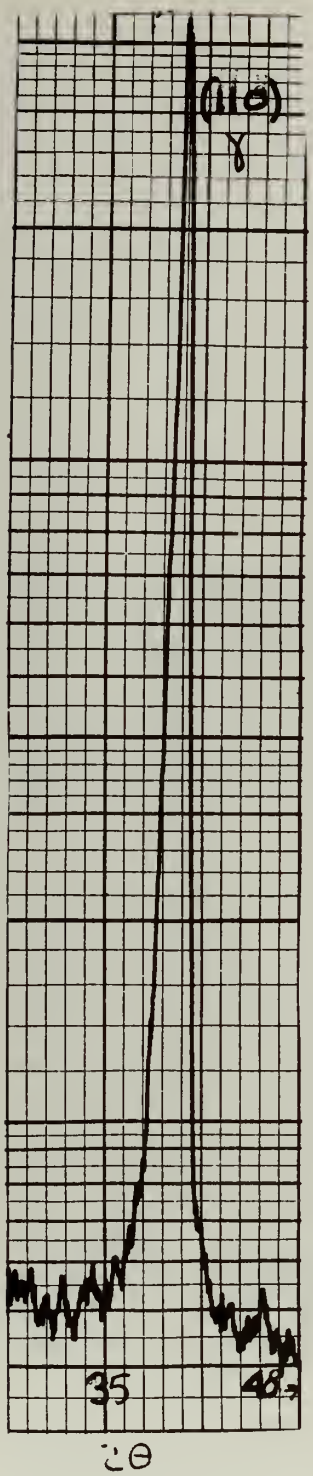

Figure 13 X-Ray Diffractometer Pattern of Control Sample, vicinity (110) gamma peak

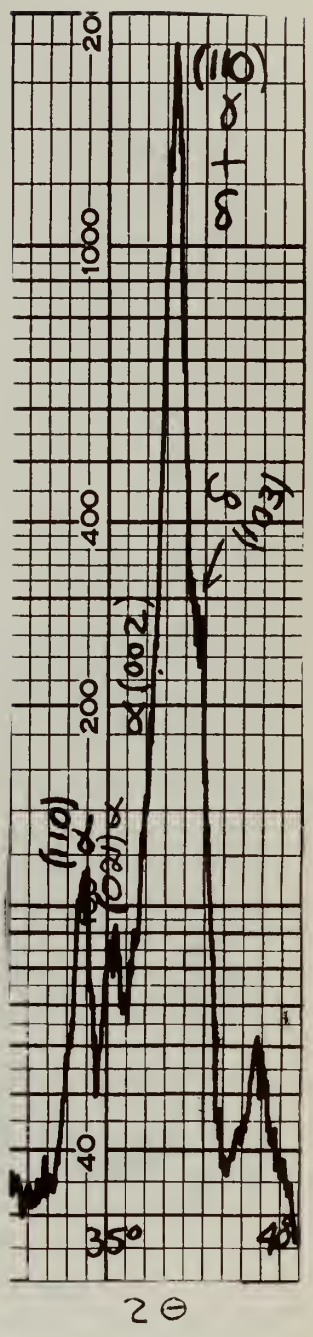

Figure 14 X-Ray Diffractometer Pattern of 315 Hour Sample, vicinity (110) gamma peak

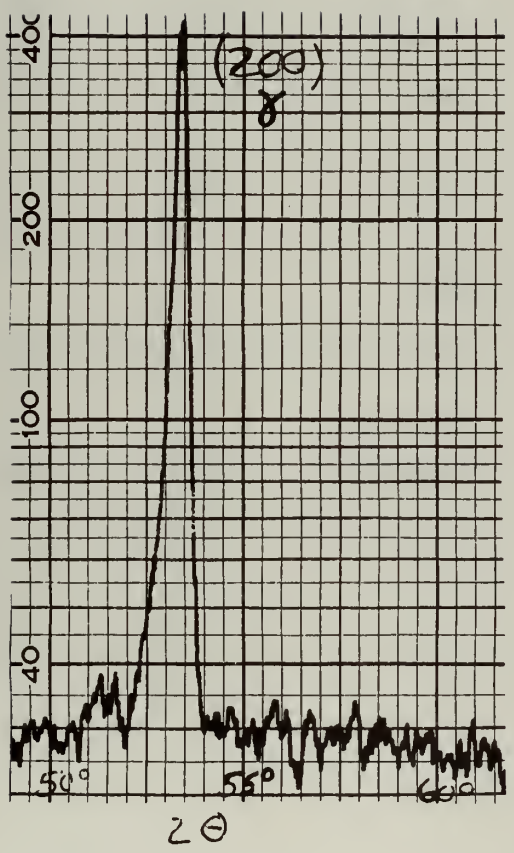

Figure 15 X-Ray Diffractometer Pattern of Control Sample, vicinity (200) gamma peak

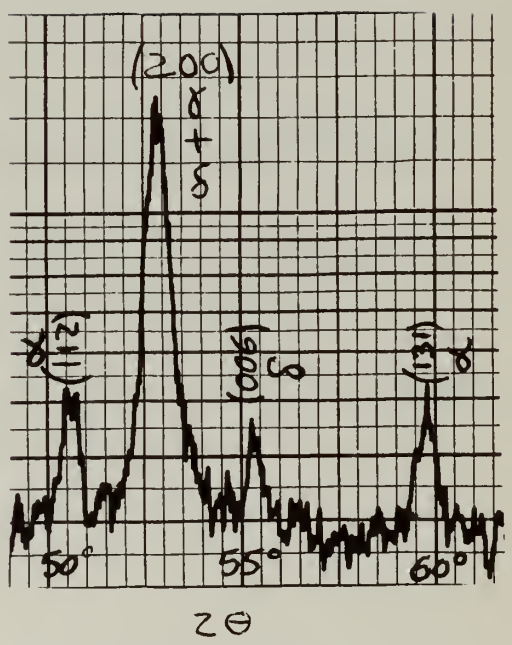

Figure 16 X-Ray Diffractometer Pattern of 315 Hour Sample, vicinity (200) gamma peak

TABLE IV-3

Diffractometer Results in Region 2Θ = 30° ⟶ 40°

for 315 Hour Sample

Peak	2Θ	d Value Observed	Identity	Remarks
110	34.9	2.569	α	
021	35.7	2.513	α	
002	36.5	2.46	α	Cannot distinguish between these three
110	37.2	2.42	γ	
110	37.2	2.42	δ	
103	37.7	2.384	δ	Visible in right of 110γ peak
111	39.3	2.29	α	

TABLE IV-4

Diffractometer Results in region 50° ⟶ 60° for 315 Hour Sample

Peak	2Θ	d Value Observed	Identity	Remarks
112	51.1	1.786	α	
200	53.3	1.717	$\gamma + \delta$	Cannot distinguish
006	55.7	1.648	δ	
131	60.3	1.534	α	

Tables App.-IV-5 and App.-IV-6 in the appendix list the complete set of "d" values and identifications thereof for the control and the 315 hour samples.

Lattice Constant Gamma Phase

Using equation (3) and the control data from Table App.-IV-5 in the appendix, the value of the lattice constant (a) was found to be 3.416 for the U-Mo lattice.

h,k,l	d Å	a Å
411	0.8052	3.4156
400	0.8541	3.4164
321	0.9133	3.4157

The results here agree with those obtained by the back deflection Laue method, that some of the sample has transformed from γ to $\alpha + \delta$. The question still exists as to whether or not possible diffusion of molybdenum and carbon has had a part to play in this transformation.

IV-C. MICROHARDNESS STUDIES

When the gamma phase transforms to alpha plus delta it behaves in a manner similar to austenitic iron transforming to ferrite plus pearlite. Thus the transformation begins at the gamma phase grain boundaries. Figure 34 shows the lamellar structure which formed on the 315 hour run. This structure is similar to the lamellar make up of pearlite in the iron system. As in the iron system the transformation of gamma to alpha plus delta should result in increased hardness.

It has been shown that X-ray diffraction is the best method of detecting transformation in the U-Mo system, but hardness readings are also used. X-ray diffraction will detect the presence of a transformed region sooner than the increased hardness will. Hardness readings were taken in order to supplement the X-ray data, and to correlate the width of the transformed region with length of run. Microhardness readings were taken using a Tukon Hardness Tester with a 136 degree diamond. The results obtained are shown plotted in Fig. 17 through 20.

The Diamond Pyramid Hardness Number is plotted versus the distance in millimeters from the hottest section of the specimen. Also shown are the surface temperatures of each specimen at each point along the specimen. The control specimen was never exposed to the thermal gradient, and is shown to establish the starting hardness.

The temperature curve marked "center line" indicates what the specimen temperature was at the center during the run. This information

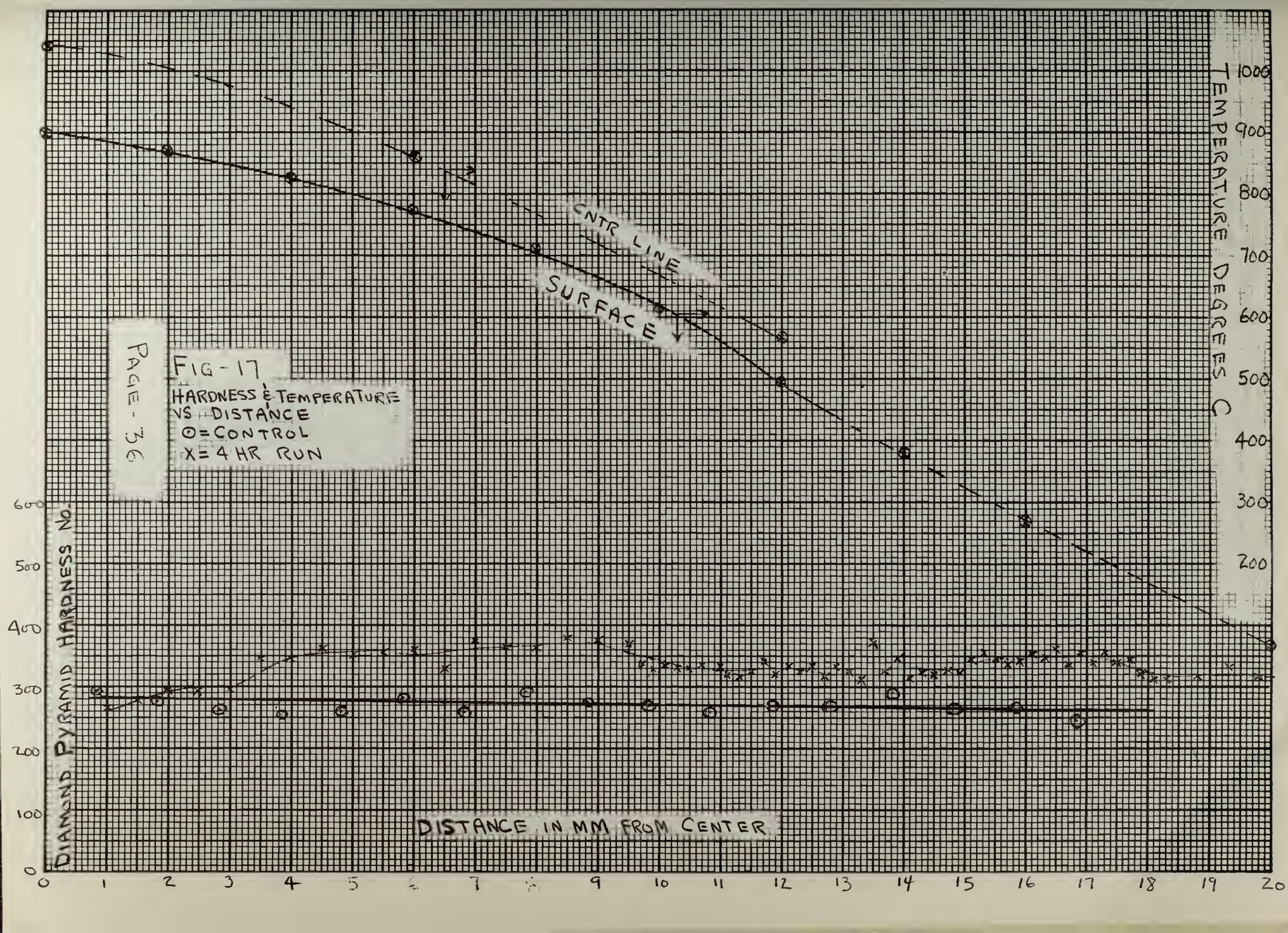

PAGE - 36

FIG - 17

HARDNESS & TEMPERATURE VS DISTANCE

⊙ = CONTROL

X = 4 HR RUN

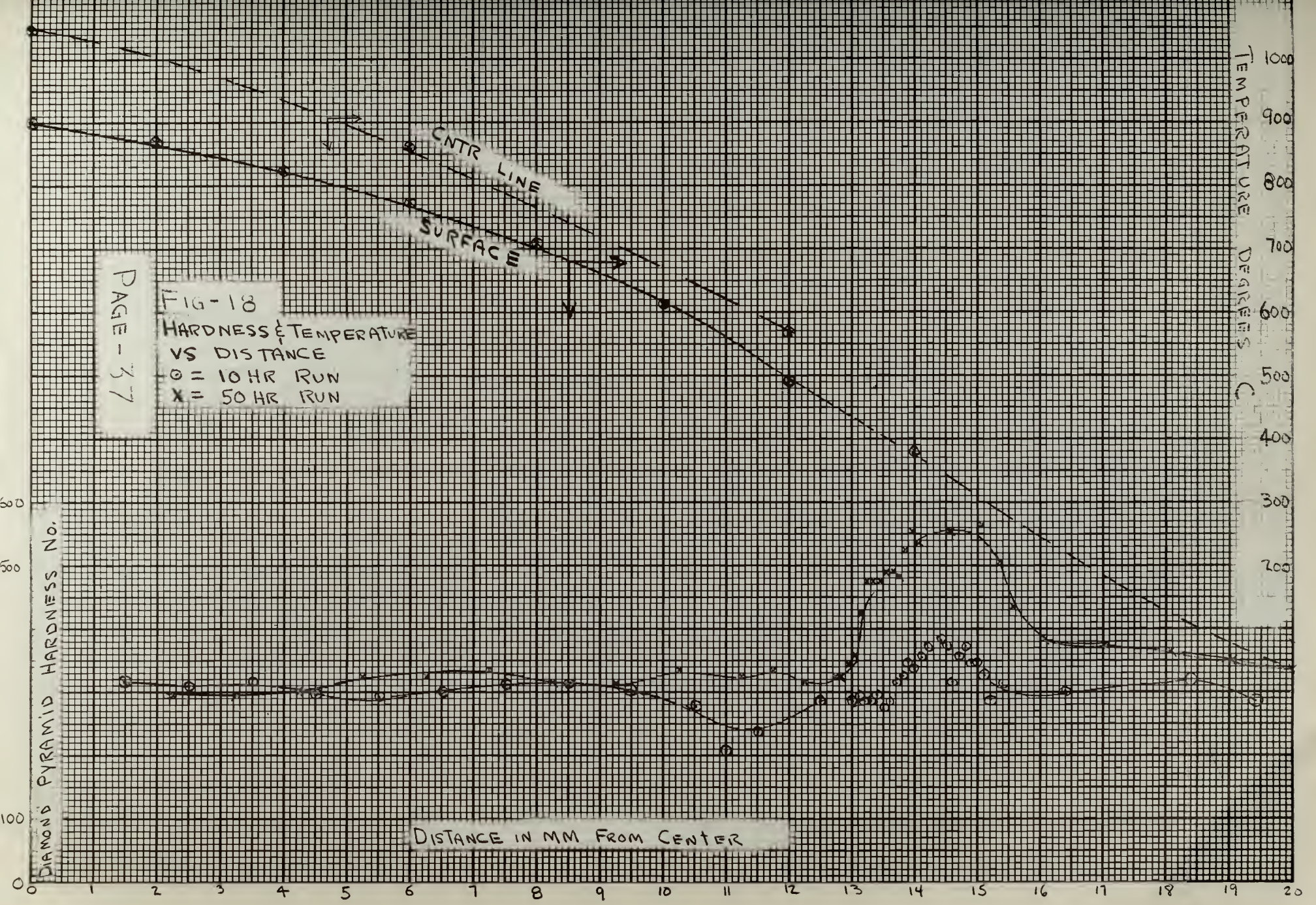

PAGE - 37

FIG - 18
HARDNESS & TEMPERATURE
VS DISTANCE
⊙ = 10 HR RUN
X = 50 HR RUN

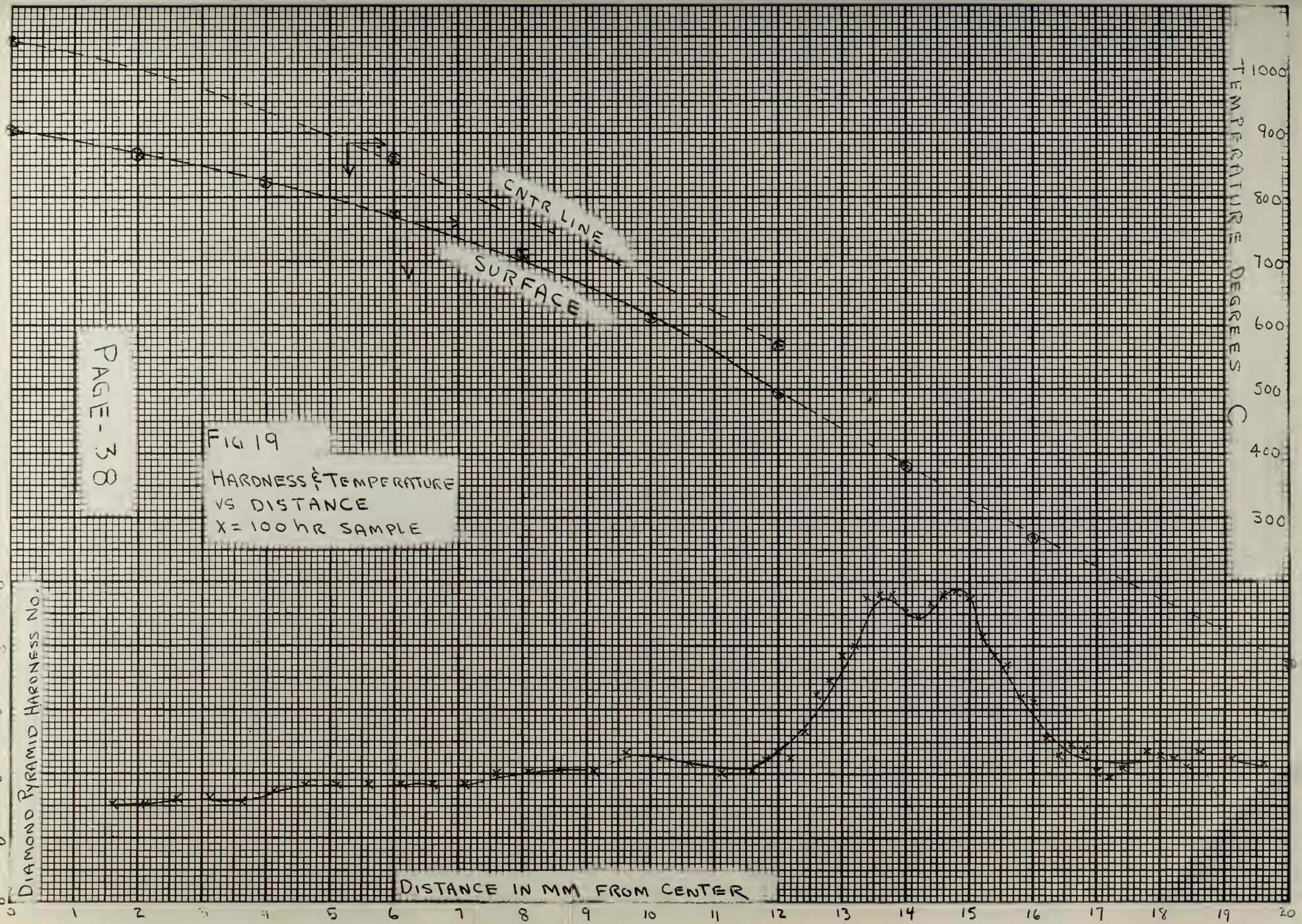

FIG 19

HARDNESS & TEMPERATURE VS DISTANCE
X = 100 HR SAMPLE

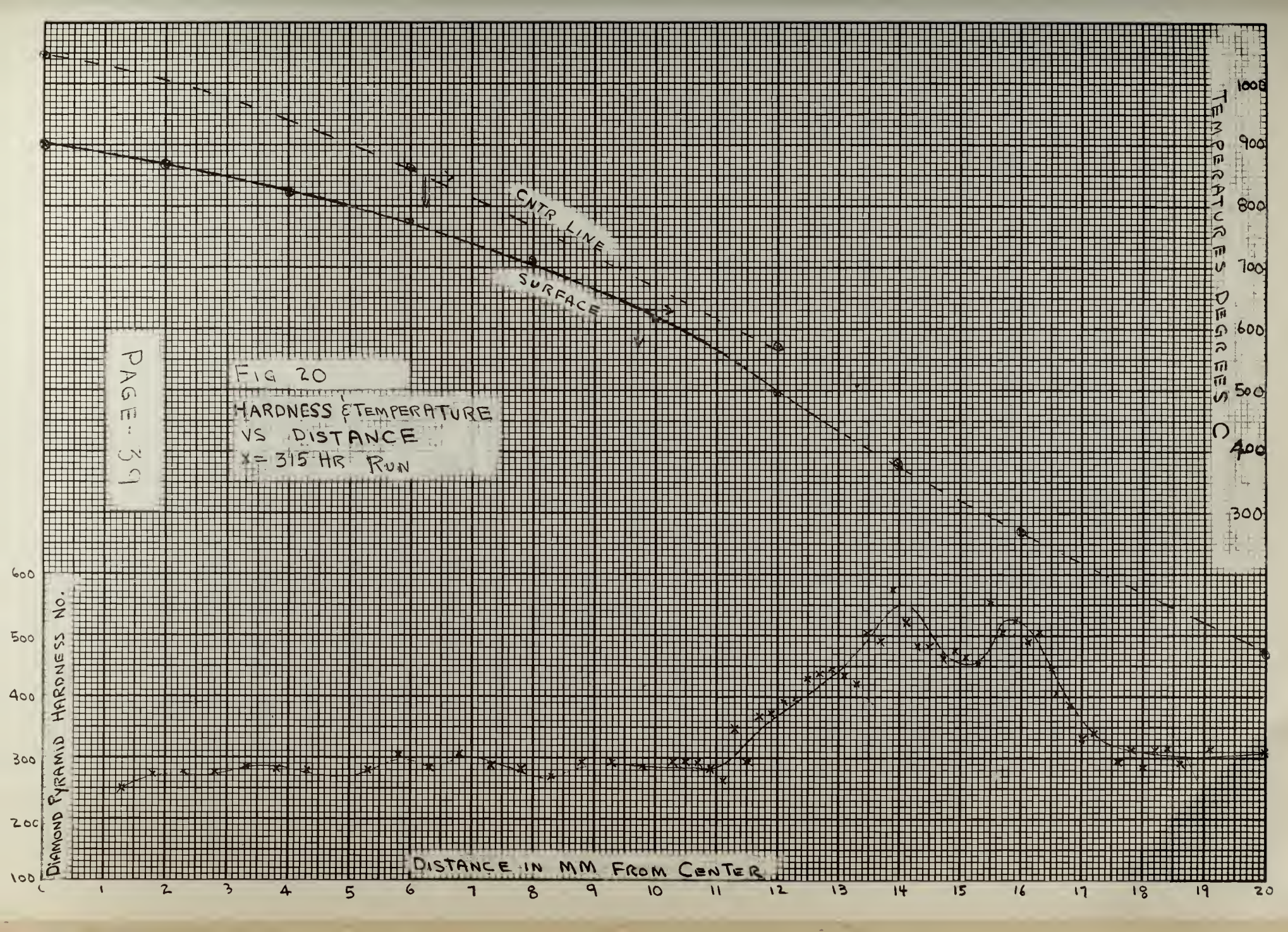

PAGE 351

FIG 20

HARDNESS & TEMPERATURE VS DISTANCE X = 315 HR RUN

was obtained from a specimen which had been specially prepared. Holes were drilled in the specimen along its length. The holes were made large enough to allow the thermocouple junction to fit into the hole, and rest on the axial center line of the specimen. In this way surface and center line temperatures were obtained along the specimen's length. Note that the surface to center line temperature difference is greatest in the region where the specimen was the hottest. This difference is due to the radiation losses from the specimen's surface. Although these losses could have been minimized by using radiation shields, the specimen would not have been visible. In order to observe the specimen during the run, and to be able to check thermocouple readings against optical pyrometer readings the radiation shields were not used.

No attempt has been made to fair a curve through the points obtained from the hardness readings for each specimen. The points themselves are close enough together to almost form a curve and have been joined for the sake of clarity. Note that the hardness does increase in the transformed region, and that the width of the harder region is dependent upon the length of time the specimen remained in the temperature gradient. Even though transformation has been detected on the four hour run by other means it is hardly detectable from the hardness data. Results of hardness for the two hour run are not shown even though some transformation had occurred since it was not detectable from the hardness data.

IV-D. METALLOGRAPHIC STUDIES

Metallographic work was performed on all samples to view the grain size and structure and to note any transformation effects.

The polish used on all samples was paper polish (320 to 4/0), fine polish with Linde A and 10% oxalic acid. Etching on all samples except the 315 hour sample was chemical in a bath of 50% H_2SO_4, 50% HNO_3, 5% HF for 10 to 15 seconds.

The 315 hour sample was electropolished in a 1 part chromic, 18 parts acetic bath at 20 volts for 1 minute. This sample was also later chemically etched for comparison with the other samples.

The results of the metallography can best be explained by reference to the photomicrographs taken.

Figure 21 is representative of any area in the control sample, polarized light, 100×. Figures 22 - 24 are from the 4 hour sample and are all polarized light at 100×. Figures 25 - 27 are from the 100 hour sample and are all polarized light 100×. Figures 28 and 29 are from the 315 hour sample and are all polarized light at 100×. Figures 30 and 31 are from the 4 hour sample and are bright light 500×. Figures 21 through 31 were all taken after the chemical etch previously described. This etch produced an oxide coating which gave a polarizing effect even in the gamma region. Figures 32, 33, and 34 were taken after the electro-polish and are bright light. Figures 32 and 33 are at 100×, and Fig. 34 is 500×.

Refer to Figure 8 for location of photomicrographs on the sample.

TABLE IV-5

Photomicrograph Data

Fig.	Hours at Gradient	Region (See Fig. 8)	Approx. Temp. °C	Comments (in all figures the left side of pictures is at higher temperature than the right side)
21	0	any	-	Control
22	4	4	800 - 900	Seems relatively free of inclusions
23	4	2	450 - 550	Transformation actually begins to right of photo(not shown)
24	4	1	50 - 100	Same as control
25	100	4	850 - 950	Note extremely large grains
26	100	2	450 - 550	Whitish area at right of picture is transformation ($\alpha + \delta$) region
27	100	1	50 - 100	Same as control
28	315	3 to 4	750 - 850	Inclusions seem to be migrating to colder region
29	315	2	450 - 550	Note transformed area more dense than Fig. 26; also great concentration of inclusions
30	4	2	450 - 550	Shows initiation of $\alpha + \delta$ in gamma grain boundaries
31	4	2	450 - 550	Taken to right of Fig. 30 (colder) shows greater growth of $\alpha + \delta$ phase
32	315	3 to 4	750 - 850	In all gamma region
33	315	2	450 - 550	Black area at right is $\alpha + \delta$ region. Note greater inclusion content than Fig. 32

TABLE IV-5 Continued...

Fig.	Hours at Gradient	Region (See Fig. 8)	Approx. Temp. °C	Comments (In all figures the left side of pictures is at higher temperature than the right side)
34	315	2	450 - 550	Shows lamallae typical of eutectoid region

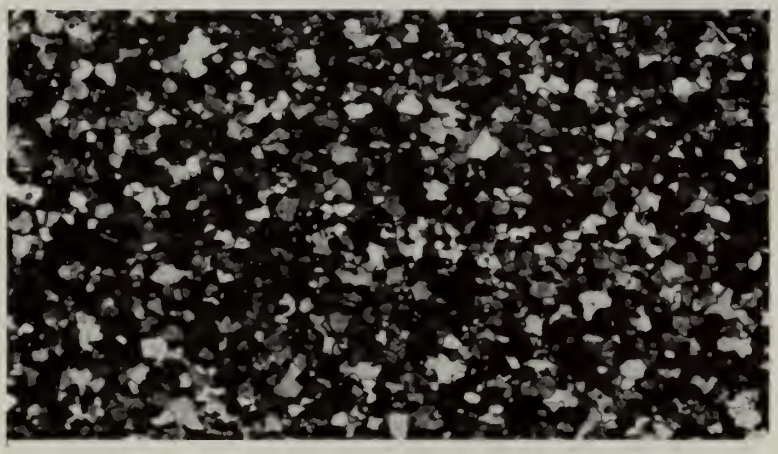

Figure 21 Control Sample
Polarized Light 100 X (20°C)

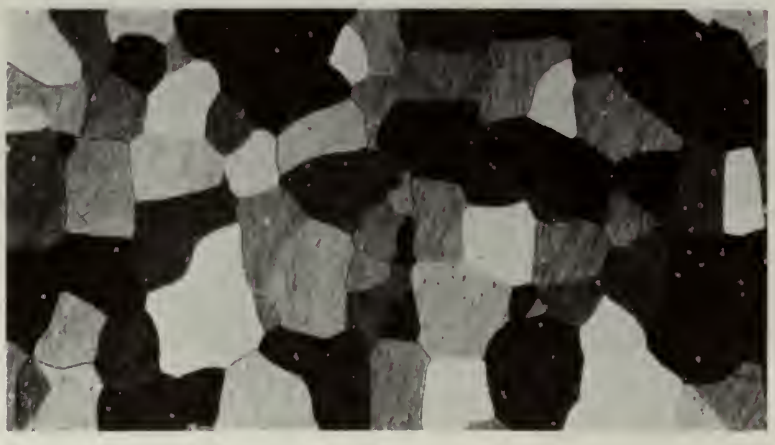

Figure 22 4 Hour Sample
Polarized Light 100 X (800°-900°C)

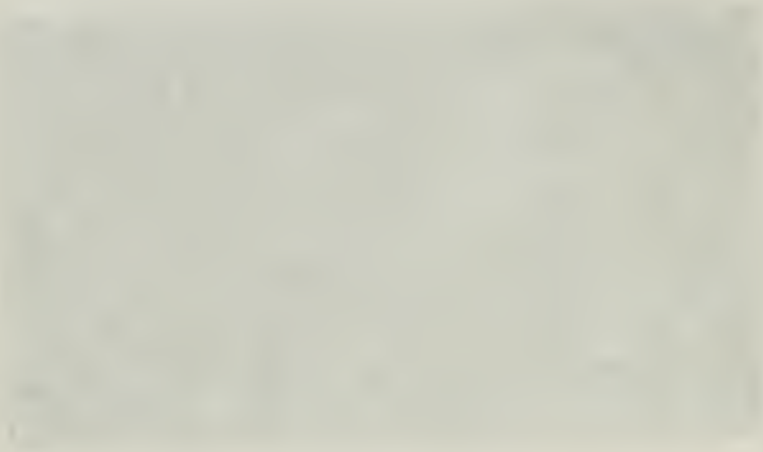

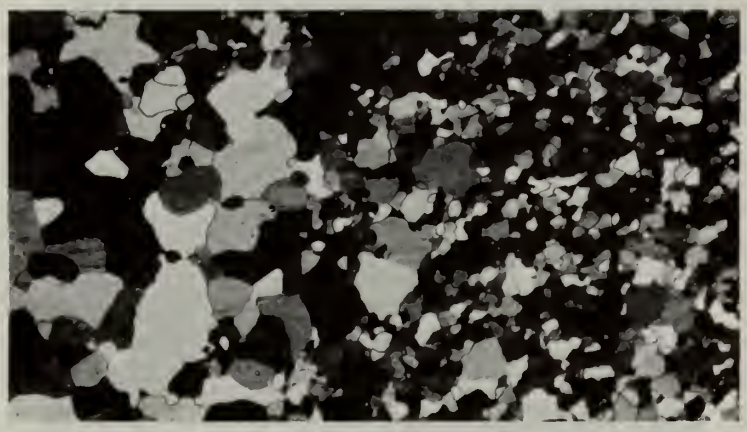

Figure 23 4 Hour Sample (450°-550°C)
Polarized Light 100 X

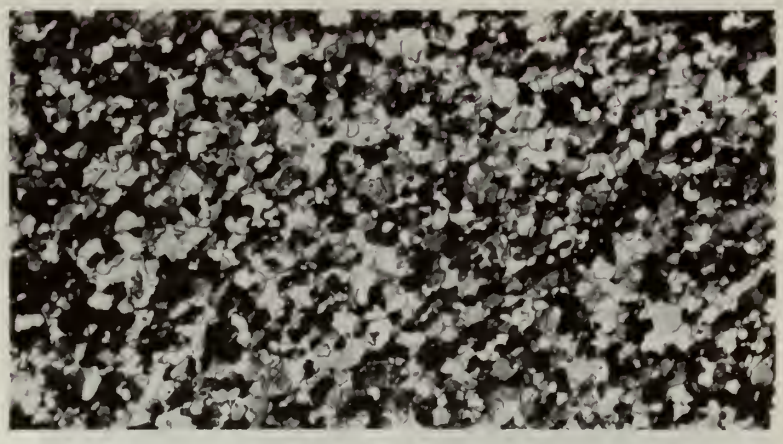

Figure 24 4 Hour Sample (50°-100°C)
Polarized Light 100 X

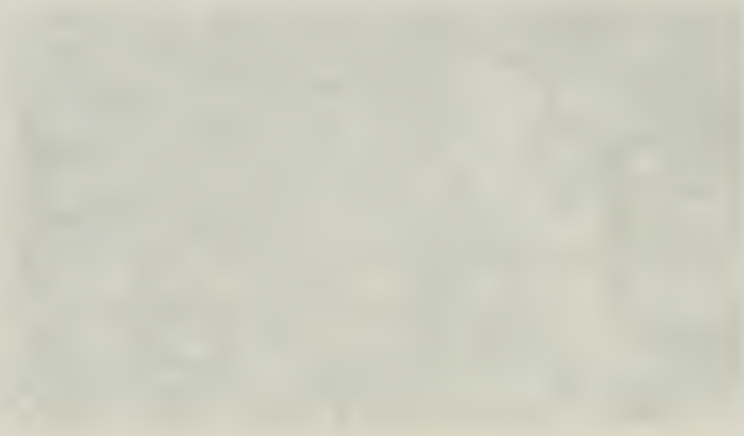

Figure 25 100 Hour Sample (850°-950°C)
Polarized Light 100 X

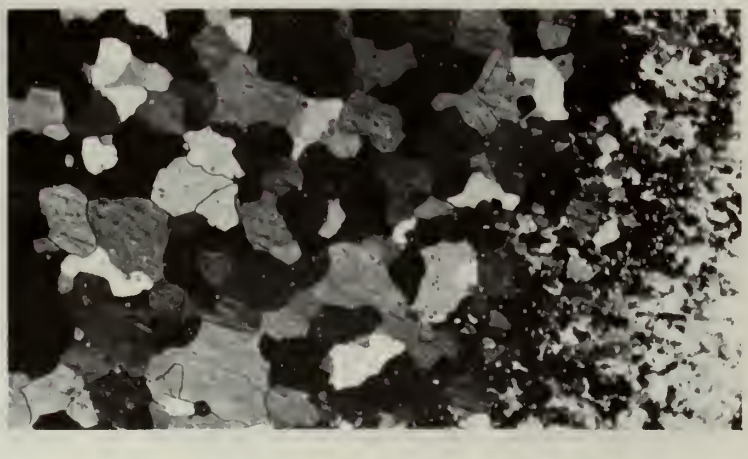

Figure 26 100 Hour Sample (450°-550°C)
Polarized Light 100 X

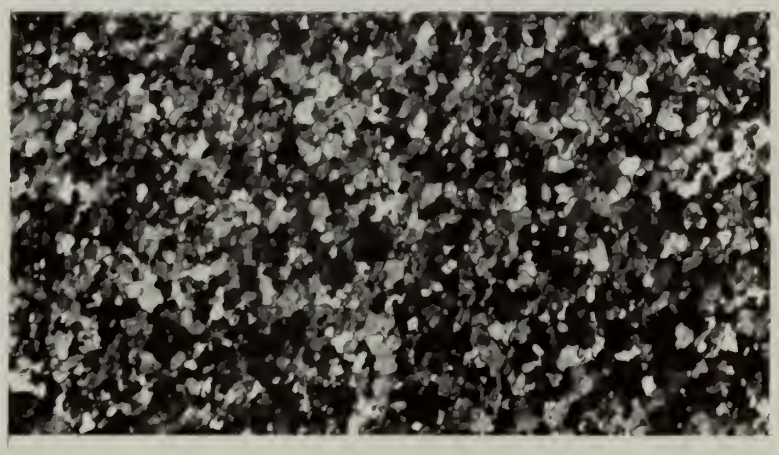

Figure 27 100 Hour Sample (50°-100°C)
Polarized Light 100 X

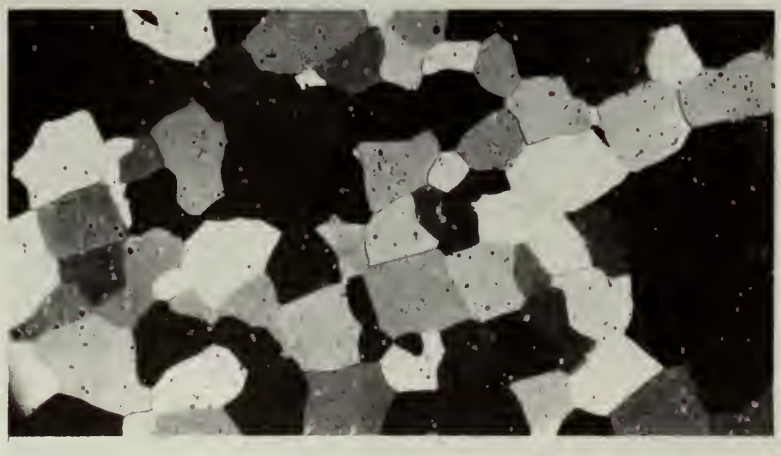

Figure 28 315 Hour Sample (750°-850°C)
Polarized Light 100 X

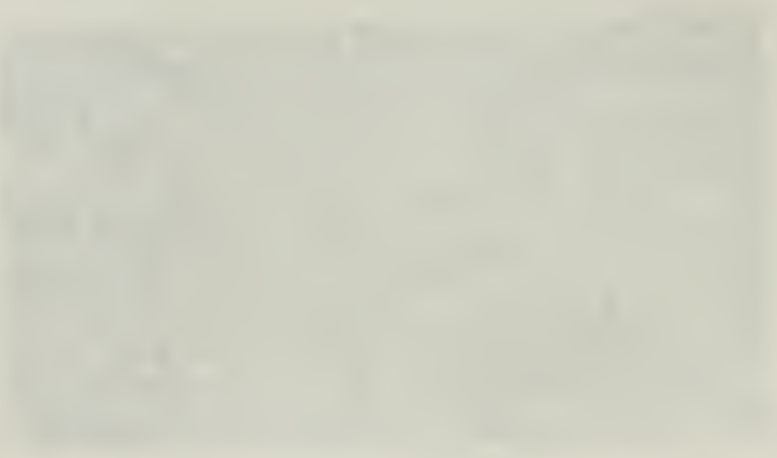

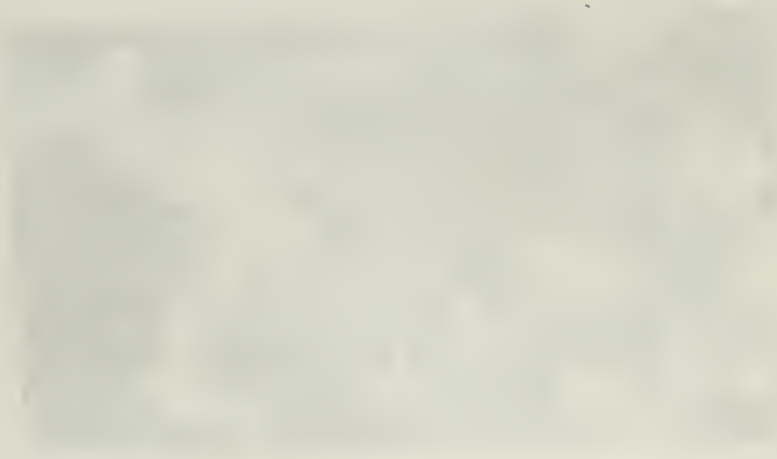

Figure 29 315 Hour Sample (450°-550°C)
Polarized Light 100 X

Figure 30 4 Hour Sample (450°-550°C)
Bright Light 500 X

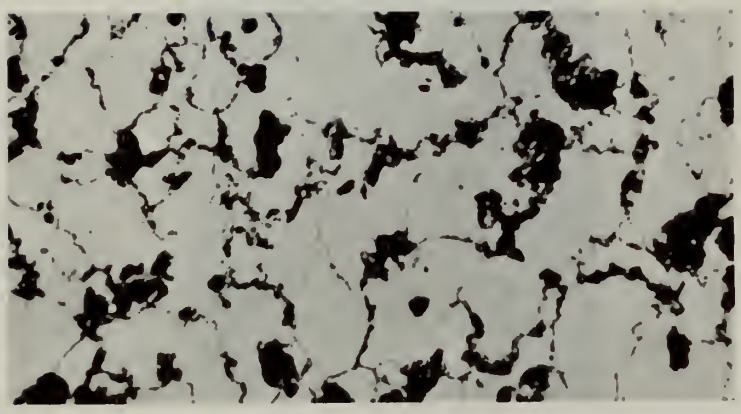

Figure 31 4 Hour Sample (450°-550°C)
Bright Light 500 X

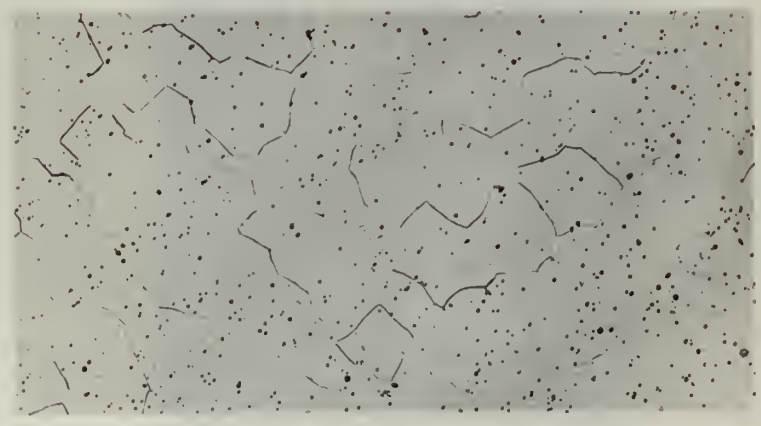

Figure 32 315 Hour Sample (750°-850°C)
Bright Light 100 X

Figure 33 315 Hour Sample
Bright Light 100 X
(450°-550°C)

Figure 34 315 Hour Sample
Bright Light 500 X
(450°-550°C)

Table IV-5 lists the photomicrographs. Important features to note are: (1) The extremely large grains in the hot central region; (2) The high density of inclusions in the transformation region of the long time sample; (3) The growth of the transformation region is such that at 315 hours (Fig. 29) its hot boundary has no small grains to its left, only the large grains. Contrast this with the 4 hour sample (Fig. 23) where there are still small grains remaining; (4) The transformation $\gamma \longrightarrow \alpha + \delta$ begins at grain boundaries (Fig. 30 and Fig. 31). The transformation product exhibit the lammelar structure characteristic of a eutectoid.

All specimens were viewed at 100× magnification for the width of the transformation region and the extent to which the gamma grains had been consumed. These results are tabulated in Table IV-6.

It should also be noted that the transformation regions were "c" shaped as shown below due to the radial temperature gradient.

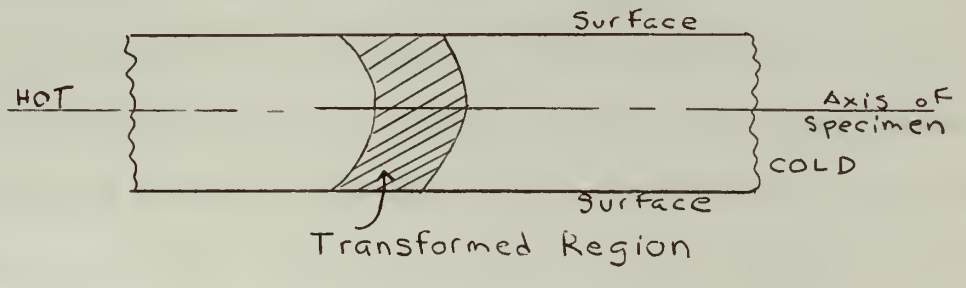

TABLE IV-6

Growth of $\alpha + \delta$ Transformation Product

Sample Hours	Amount of Coverage, %	Width, m.m.
2	30	1.91
4	50	2.29
10	70	2.66
50	100 (except in immediate boundaries)	3.01
100	100 (except in immediate boundaries)	3.39
315	100 (except in immediate boundaries)	4.64

This data was plotted on a log-log plot (see Fig. 35) and a straight line was faired through the points. The equation of this line is $d = 1.96t^{0.134}$ where "d" is the width in mm and "t" is the time in hours. It is assumed that this curve would eventually approach a horizontal line if additional long time data had been taken. Here $d = d_{max}$ independent of time.

Note that Fig. 35 and Table IV-6 show transformation occurring at times as short as two hours. Figure 2, on the other hand, indicates that a minimum of 22 hours is required at approximately 500°C before transformation will begin. This contradiction is easily explained. The data of Table IV-6 resulted from exposing the specimen to a thermal gradient for the times indicated. Figure 2 was derived from tests in which each specimen was held at a fixed temperature for the times indicated, and

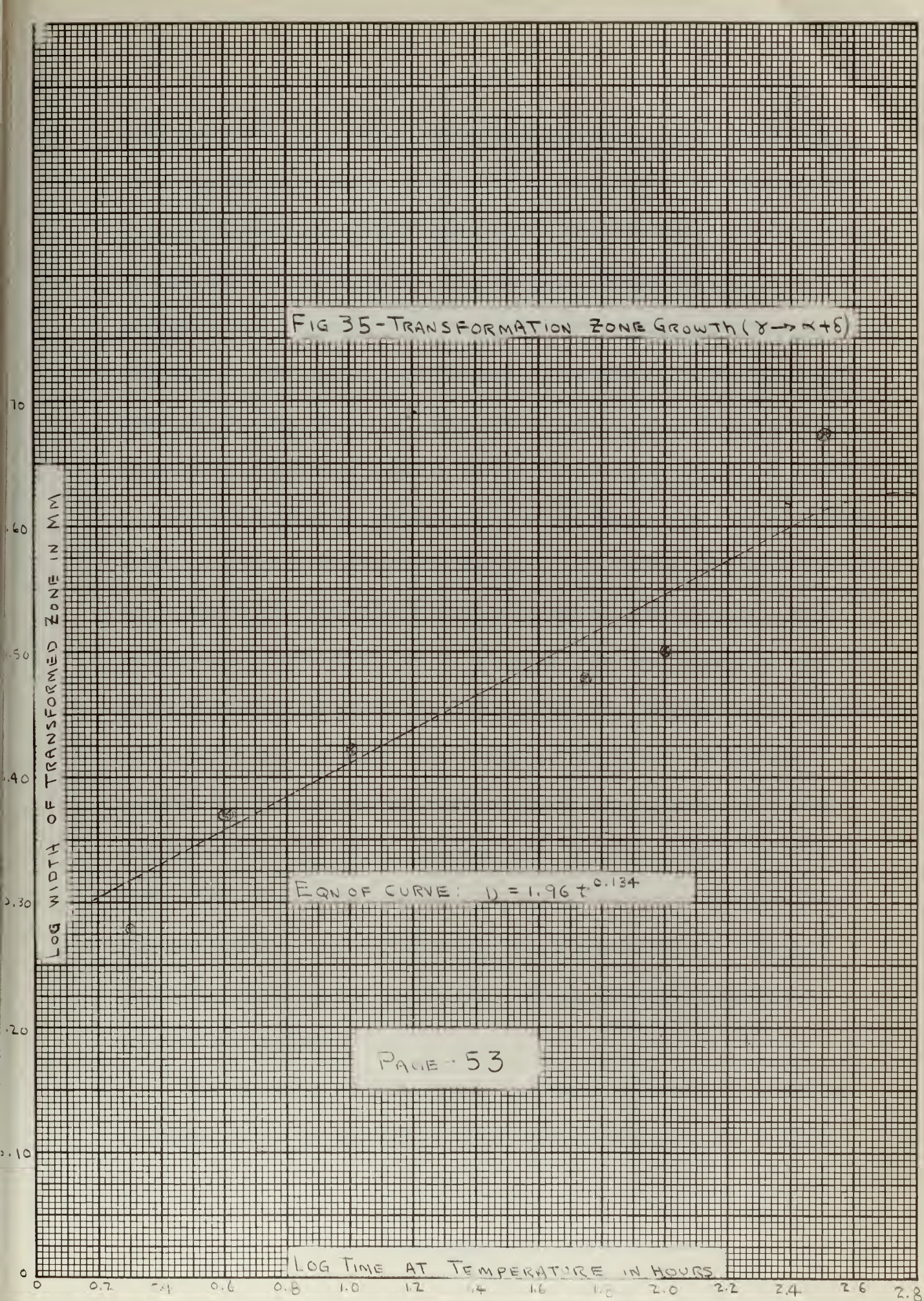
FIG 35 - TRANSFORMATION ZONE GROWTH (γ → α + δ)
LOG WIDTH OF TRANSFORMED ZONE IN MM
EQN OF CURVE: D = 1.96 t^0.134
LOG TIME AT TEMPERATURE IN HOURS
0
0.2
0.6
0.8
1.0
1.2
1.6
2.0
2.2
2.4
2.6
2.8
.10
.20
.30
.40
.50
.60
70

then analyzed. In addition, the prior history of the specimen used in obtaining the data for Fig. 2 was not the same as that for the specimens used in obtaining the data of Table IV-6. Impurity content of the specimen can also have a marked effect upon the time required for the initiation of transformation. Pickleshimer[4] points out that a small amount of impurities (330 ppm C, 500 ppm Fe, and 250 ppm Si) can cuase the transformation to occur sooner than expected.' He observed initial transformation starts much sooner than those reported on Fig. 2, and he suspects the greater amount of impurities he had present were the cause. Van Thyne[1] reports differences due to cold work on hardness. He reports cold swaging causes the beginning of observable increases in hardness to occur at a much earlier time. Essentially then, Pickleshimer and Van Thyne give two effects which shift the nose of the TTT curve to the left. Another factor which is undoubtedly of major importance is that all of the work previously reported has been of two types (a) the direct step quench, (b) quench and reheat where all of the specimen is at the same temperature at any given time. Even these methods do not give consistent transformation kinetics results. The decomposition of a solid solution is different depending on the method involved and differences in transformation kinetics are expected.

The method of using a thermal gradient to analyze transformation initiation is new to the field of transformation kinetics. The gradient

method also allows the full range of temperatures to be present in a single specimen and hence provides a continuous distribution of any transformations for the time during which the gradient was applied.

It is, therefore, justifiable that these transformation kinetics results should differ due to the fact (a) that a large number of inclusions (probably carbon) have migrated toward the transformation region from the hot end; (b) there was a large amount of cold swaging performed in the specimen's prior history; (c) this method is physically different. Actually it is possible that the results reported here may be closer to what actually takes place in the fuel pin in the operating Fermi Fast Breeder Reactor (except for the effect of the radiation flux) since the fuel pins are to be swaged even more than the specimens used here, and they will be subjected to thermal gradients similar to those used in this study.

IV-E. DIFFUSION STUDIES

Molybdenum

It seemed conceivable at the inception of the experimental part of the work that the existence of the steep temperature gradient might lead to some detectable movement of the molybdenum, enriching one area and depleting another area of the fuel pin. As yet theoretical work substantiating or refuting this has not been developed. Fick's Laws of diffusion are not readily applicable in this situation where a temperature gradient is maintained.

It was decided to check several of the specimens for any movement of the molybdenum since a depletion of the molybdenum in any area (below 10% w/o) would have serious consequences if it allowed the gamma phase to transform to the alpha during the operation of a reactor.

Since any movement would be expected to be of the order of microns, it was decided that the best method to use to detect it would be via a microbeam probe. Consequently, beam probe analyses were performed on the control, 4 hour, 100 hour and 315 hour samples. The following results were noted: control sample and 4 hour treatment:- these were run manually across the specimen in jumps of 0.010" in the cold and hot area, and steps of 0.001" in the region of the steepest gradient with results giving a molybdenum concentration across the sample which was 10.0% $\pm$ 0.3%. The 100 hour and 315 hour samples were run on motor scan and the results were 10.0% $\pm$ 0.4%. It should

be noted that both of these are written in the form X ± Y where X is the 10% or mean value and Y is the standard deviation.

These values would seem to be consistent with the report[13] submitted by Nuclear Metals, Inc., to Power Reaction Development Corporation concerning its studies on homogeneity in the Fermi Fast Breeder Reactor fuel pins.

The fact that diffusion was not observed after 315 hours should not be considered conclusive that it will never occur.

Carbon

A careful study of the photomicrographs obtained in the metallographic studies of the specimens indicated that carbon diffusion might be occurring. It appeared that there were less inclusions in the region of the hot zone than in the transformed section. Pickleshimer[4] pointed out that the presence of impurities caused transformation to occur sooner than expected in the U-Mo system. If carbon did diffuse from the hot zone to the shoulder(see Fig. 8, region 2), it could be aiding the early initiation of transformation.

In an attempt to substantiate the visual observations made, and those results derived from the photomicrographs it was decided to analyze the specimen for carbon. The 100 hour and 315 hour specimens were each sectioned into three pieces. A cold section, a shoulder section, and a hot section. These sections were subjected to

destructive tests for carbon analysis. The results of the analysis were not conclusive. To obtain conclusive results larger size samples would be necessary, and were not available. Therefore, substantiation of the observed data is not available, and it cannot be definitely stated that the carbon diffused.

V. CONCLUSIONS AND RECOMMENDATIONS

A. Transformation Kinetics

Using data as given in APDA 124, and the results as found in this work, a temperature gradient and growth of transformation region plot was made for the Fermi Fast Breeder Reactor. Data from APDA 124 appears in Table V-1.

TABLE V-1

Temperature Distribution Fermi Reactor

Position	Nominal Temp. °F	°C	Remarks
(Fuel Pin U-Mo Diameter 0.148", U-10% w/o Mo, with cladding)			
(a) Center line U	1134	612	Hottest pin of central
Clad-Fuel interface	930	499.5	fuel subassembly
(b) Center line U	798	425.5	Hottest pin of coolest
Clad-Fuel interface	710	376.5	fuel subassembly
Blanket Rod (U-Mo diameter 0.415", U-2.75% w/o Mo)			
(c) Axial			
Center line U	1023	550	Hottest rod of axial
Fuel-Na interface	940	505	blanket
(d) Radial			
Center line U	1041	560	Hottest rod of radial
Fuel-Na interface	800	427	blanket

Figure 36 a shows expected region of transformation γ + δ for the central fuel pin. Transformation would begin at the circumference

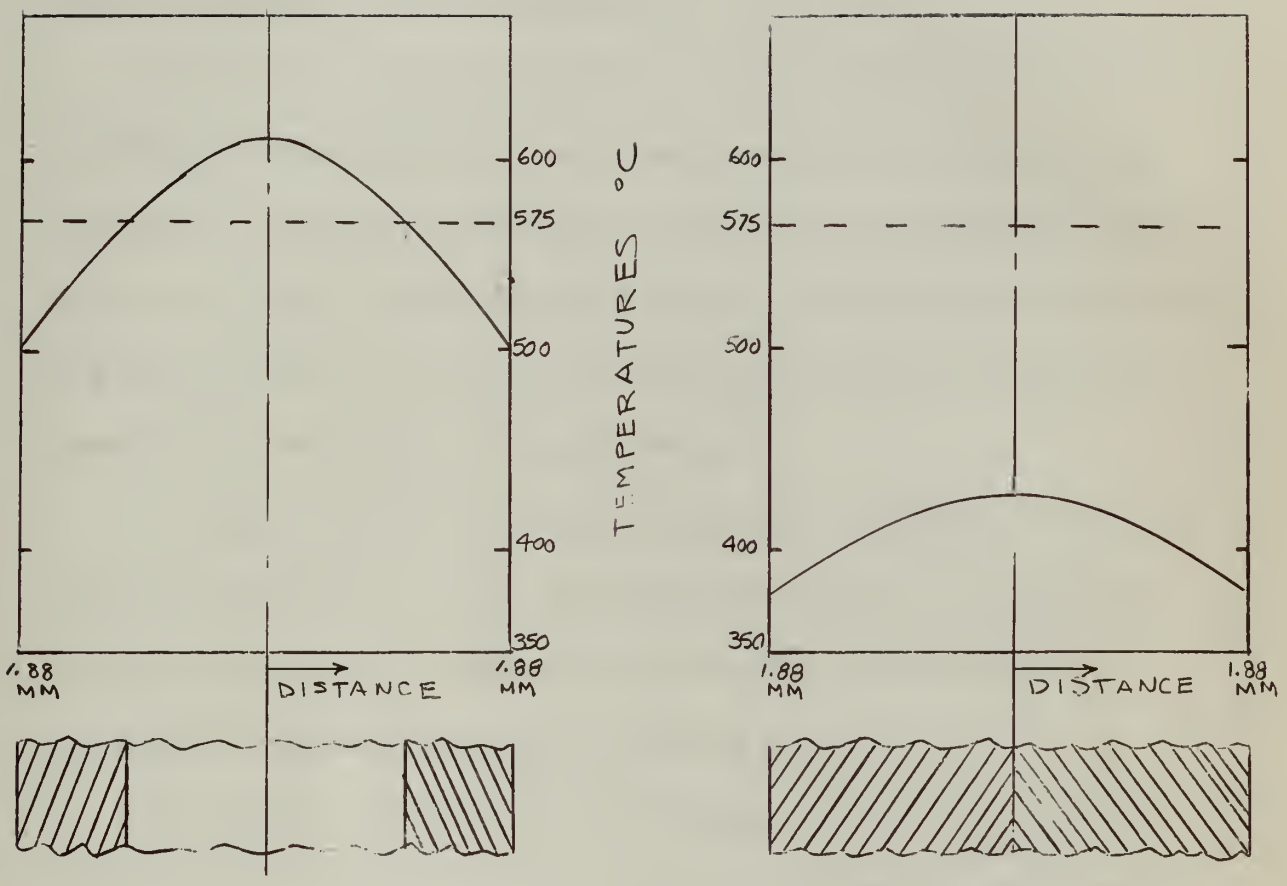

Note: Shaded Areas Indicate Completed Transformation $\gamma \rightarrow \alpha + \delta$
1.88 mm is distance to fuel-clad interface.

Fig. 36 a

Radial temperature and transformation distribution for hottest fuel subassembly. Completion of transformation estimated at 50 hours.

Fig. 36 b

Radial temperature and transformation distribution for coolest fuel subassembly. Completion estimated at 10 hours.

Fig. 36. Estimated Temperature and Transformation Region Distribution in Two Fermi Fast Breeder Reactor Fuel Pins. (Effects of radiation not taken into account.)

and work its way in toward the center to the point where the temperature is approximately 575°C. After sufficient time (estimated at 50 hours) the transformed region would be as shaded.

At the other extreme is Fig. 36 b, for the coolest fuel subassembly. Here transformation begins at the center line and works its way toward the outside, eventually (approximately 10 hours) transforming the entire fuel pin as shown. At intermediate fuel pins, transformation would begin at a point between the centerline and circumference and would proceed toward the center and the surface of the pin.

It must be pointed out that the above in no way takes into account the effects of radiation on the transformation kinetics. It is expected that this effect will slow down the transformation, and such an investigation should follow the work started here.

It should be noted that the Fermi Reactor blanket rods containing only a U-2.75% w/o Mo alloy will transform to alpha plus delta uranium much sooner than the U-10% w/o Mo alloy. Recognizing this, an allowance was made in the design of the blanket rods for expansion due to thermal effects and irradiation growth effects on the transformed alpha uranium. It is evidently expected that irradiation will have but little effect on the transformation kinetics of this alloy.

In summation, it has been found that this alloy definitely transforms to the undesirable alpha plus delta state in a relatively short time at reactor operating conditions. A corollary result of this work is that a

gradient furnace such as used here would provide a new method of studying transformation kinetics, in that a complete range of temperatures exists in a given specimen at any one time.

B. Carbon and Molybdenum Diffusion

The thermal gradient did not produce any molybdenum segregation in this study. Results of microbeam probe analysis showed that no molybdenum diffusion has occurred in specimens held in a 1900°C per inch thermal gradient. The longest run was for a period of 315 hours. It is, therefore, possible that molybdenum may still diffuse during the life time of the fuel pin. In the reactor the fuel pins are exposed to thermal gradients as high as 1500°C per inch and fuel pin life is much longer than 315 hours.

An attempt was made in this study to determine whether carbon had diffused from one particular region. Visual observations of the specimens at 100× and 500× showed a depletion of inclusions in the hot region. The photomicrographs also show fewer inclusions in the hot zone than exist in the transformed region. Chemical analysis of various sections of the specimens was attempted, but the results were not conclusive. It cannot definitely be stated, as a result of this study, that the carbon diffused.

As a result of this study, the following is recommended:

1. A diffusion furnace be built to attain thermal gradients much higher than the 1900°C per inch used in this study.

2. Additional experiments be carried out on the uranium-10% w/o molybdenum and other fuel element alloys at times greatly in excess of 315 hours to determine the effects of such gradients on diffusion and transformation kinetics.

3. Repeat the experiments in 2 in a radiation field to determine what stabilization effects, if any, occur.

APPENDIX

SECTION A

TABLES OF DATA REFERENCED IN SECTION IV-B

TABLE APP.-IV-1

Tabulated Values of "d" for δ Phase U-Mo Alloys

h, k, l Tucker	Multiplicity P	Intensity	d Observed Å	h, k, l Halteman*
110	4	S	2.44	110
101	8	VS	2.39	103
200	4	S	1.717	200
002	2	M	1.646	006
211	16	VS	1.390	213
112	8	M	1.347	116
220	4	MW	1.213	220
202	8	MW	1.184	206
310	8	S	1.080	310
301	8	-	-	303
103	8	MW	1.041	109
222	8	M	0.972	226
321	16	M	0.911	323
312	16	M	0.903	316
123	16	M	0.889	129
400	4	MW	0.854	400
004	2	VW	0.819	0, 0, 12
411	16	S	0.804	413
330	4	-	-	330
303	8	MS	0.790	309

a = 3.425
c = 3.282
} Work of C. W. Tucker, J. Inst. Met, 78, 760 (1951).

*Addendum

a = 3.427
c = 9.834
} Work of E. K. Halteman, Acta Crystal., 10, 166 (1957).

TABLE APP.-IV-2

Tabulated Values of "d" for ∝ Uranium;

Work of Jacob and Warren Appearing in ASTM X-Ray Powder Data File

h, k, l	Intensity I/I_1 %	d Å
110	100	2.563
021	100	2.521
002	100	2.473
111	100	2.274
112	100	1.778
131	100	1.532
221, 004, 202	100	1.238
135, 331, 063	100	0.843
313, 154	100	0.815
020	30	2.948
022	30	1.888
130	30	1.614
040	50	1.466
023	70	1.436
200	50	1.423
041	30	1.402
113	70	1.387
132	50	1.350
220	30	1.282
042	70	1.260
133	70	1.153
114	70	1.114
043	30	1.100
150	60	1.088
240	50	1.022
223	70	1.012
241	30	1.001
152	70	0.992
060	30	0.977
061	30	0.958

Table App.-IV-2 Continued.....

h, k, l	Intensity I/I_1 %	d Å
044 242	70	0.945
310 025 204	70	0.936
115 311	60	0.922
062	50	0.908
312	60	0.878
243	50	0.869
330	30	0.855
006	50	0.824

a = 2.852

b = 5.865

c = 4.945

CuK_{α} with Ni filter

TABLE APP.-IV-3

Back Deflection Laues

SPECIMEN - Control

Region	Description	X_{cm}	tanα	α°	180-α°	θ°	Sin θ°	Å "d" Value	Plane (h,k,l)	Material
All	Untransformed	1.98	0.66	33.52	146.48	73.24	0.957	0.8046	(411)	γU
		3.73	1.25	51.35	128.65	64.32	0.901	0.8546	(400)	γU
		6.74	2.145	65.00	115.00	57.50	0.843	0.9130	(321)	γU

TABLE APP.-IV-4

Back Deflection Laues

SPECIMEN - 100 hours

Region*	Description	X cm	tan α	α°	180°-α°	Θ°	Sin Θ	"d" Value A	Plane (h, k, l)	Material $\alpha, \delta, \gamma, U$
1	Cold end untrans-	1.98	0.66	33.52	146.48	73.24	0.957	0.8046	(411)	γ
	formed	3.73	1.25	51.35	128.65	64.32	0.901	0.8546	(400)	γ
		6.74	2.145	65.00	115.00	57.50	0.843	0.9130	(321)	γ
4	Hot end un-	1.98	0.66	33.52	146.48	73.24	0.957	0.8446	(411)	γ
	transformed	3.73	1.25	51.35	128.65	64.32	0.901	0.8546	(400)	γ
	practically single crystal pattern								(321)	not noted
3	Warm end	1.98	0.66	33.52	146.48	73.24	0.957	0.8046	(411)	γ
	above trans-	3.73	1.25	51.35	128.65	64.32	0.901	0.8546	(400)	γ
	formation zone, smaller grains than in #4 above	6.74	2.145	65.00	115.00	52.50	0.843	0.9130	(321)	γ
2	Transformation region	2.10	0.70	34	146	73	0.956	0.805	(413) δ (411) γ	γ or δ
	$\gamma \rightarrow \alpha + \delta$	2.38	0.7935	38.43	141.57	70.78	0.944	0.8154	(313) (154)	α
		3.365	1.12	48.25	131.75	65.88	0.913	0.843	(135) (331) (063)	α
		3.80	1.268	51.7	128.3	64.15	0.900	0.855	(400)	γ or δ
		5.28	1.76	60.4	119.6	59.8	0.864	0.892	(129)	δ

* Refers to Figure 8.

TABLE APP.-IV-5

X-Ray Spectrometer Data for Control Sample

CuK_{α} with Ni Filter

40 K.V., 16 Ma

Plane h, k, l	2Θ Degrees	"d" Value Observed	Material
411	146.1	0.8052	All gamma
400	128.8	0.8541	
321	115.0	0.9133	
222	102.5	0.9876	
310	90.8	1.0818	
220	79.0	1.2100	
211	66.8	1.3992	
200	53.4	1.7143	
110	36.9	2.4338	

TABLE APP.-IV-6

X-Ray Spectrometer Data for 315 Hour Sample

CuK_{α} with Ni Filter

40 K.V., 22Ma

Plane	2θ	"d" Value Observed	Tabulated*	Material Phase	Remarks
110	34.9	2.569	2.56	α	
021	35.7	2.513	2.52	α	
002	36.5	2.46	2.47	α	
110	37.2	2.42	2.438	$\gamma + \delta$	Cannot distinguish
103	37.7	2.384	2.39	δ	
111	39.3	2.291	2.274	α	
112	51.1	1.786	1.778	α	
200	53.3	1.717	1.714	$\gamma + \delta$	Cannot distinguish
006	55.7	1.648	1.646	δ	
131	60.3	1.534	1.532	α	
040	63.5	1.464	1.466	α	
023	64.8	1.437	1.436	α	
211γ 213δ	67.0	1.395	1.399	$\gamma + \delta$	Cannot distinguish
132	69.2	1.356	1.350	α	
221 004 202	76.7	1.241	1.238	α	
220	79.3	1.207	1.210	γ	
133	83.7	1.154	1.153	α	
310	89.9	1.1090	1.080	δ	
310	90.7	1.083	1.0818	γ	
109	96.3	1.034	1.041	δ	
240	97.8	1.022	1.022	α	
223	99.1	1.012	1.012	α	
241	100.8	0.9996	1.001	α	
152	102.0	0.991	0.992	α	
222	102.6	0.986	0.987	γ	
060	104.0	0.977	0.977	α	
226	104.8	0.972	0.972	δ	
044 242	109.0	0.946	0.945	α	

Table App.-IV-6 Continued....

Plane	2Θ	"d" Value Observed	Tabulated*	Material Phase	Remarks
323	115.6	0.9107	0.911	δ	
321	115.1	0.9127	0.9133	γ	
316	117.2	0.9024	0.903	δ	
129	120.1	0.8889	0.889	δ	
243	125.1	0.868	0.869	∝	
400	128.4	0.8555	0.8541	γ + δ	Cannot distinguish
135 331 063	131.8	0.8438	0.843	∝	
313 154	141.7	0.815	0.815	∝	
411γ 413δ	145.7	0.806	0.805	γ + δ	Cannot distinguish
309	154	0.7905	0.790	δ	

NOTE: 100 sample similar, but not as many ∝ or δ peaks observed.

* Jacob and Warren for ∝ .
Tucker modified by Halteman for δ .
Control specimen for γ.

APPENDIX

SECTION B

LISTING OF REFERENCES

1. Van Thyne, R. J. and McPherson, D. J., "Transformation Kinetics of U-Mo Alloys," Trans., Am. Soc. Metals, 49, 598 (1957).

2. Pfeil, P. C. L., "The Constitution of U-Mo Alloys," J. Inst. Metals, 77, 553 (1950).

3. Tucker, C. W., "Discussion of the Constitution of U-Mo Alloys by P. C. L. Pfeil in Journal of the Institute of Metals," J. Inst. Metals, 78, 760 (1951).

4. Pickleshimer, M. L., "Discussion on Transformation Kinetics of U-Mo Alloys by R. J. Van Thyne and D. J. McPherson in Transactions of the American Society for Metals," Trans., Am. Soc. Metals, 49, 619 (1957).

5. Bauer, A. A., "Discussion on Transformation Kinetics of U-Mo Alloys by R. J. Van Thyne and D. J. McPherson in Transactions of the American Society for Metals," Trans., Am. Soc. Metals, 49, 619 (1957).

6. Van Thyne, R. J. and McPherson, D. J., "Transformation Kinetics of U-Niobium and Ternary U-Mo Base Alloys," Trans., Am. Soc. Metals, 49, 576 (1957).

7. Pfeil, P. C. L. and Brown, J. D., "Superlattice Formation in U-Mo Alloys," A.E.R.E., M/R, 1333 (1954).

8. Halteman, E. K., "The Crystal Structure of U_2Mo," Acta Cryst., 10, 166-69 (March 10, 1957).

9. ASTM X-Ray Powder Data File.

10. APDA-124 (1959).

11. Rough, F. A. and Bauer, A. A., "Constitution of Uranium and Thorium Alloys," BMI-1300 (1958).

12. Bauer, A. A., "Discussion on Transformation Kinetics of Uranium, Niobium and Ternary U-Mo Base Alloys by R. J. Van Thyne and D. J. McPherson in Transactions of the American Society for Metals," Trans., Am. Soc. Metals, 49, 593 (1957).

13. Randall, R. N. and White, A. M., "Final Report to PRDC on The Investigation of Methods for Producing Homogeneity in Fuel Pin Cores," NMI-4410 (1959).

14. Wilkinson and Murphy, W. F., "Nuclear Reactor Metallurgy," D. Van Nostrand Company, Princeton, New Jersey (1958).

15. Gurinsky, D. H. and Dienes, G. J., "Nuclear Fuels," D. Van Nostrand Company, Princeton, New Jersey (1956).

16. Evans, R. D., The Atomic Nucleus, McGraw-Hill Book Company, New York (1955).

17. Barrett, C. S., Structure of Metals, McGraw-Hill Book Company, New York (1952).

18. "Atom Movements," American Society for Metals (1951).

19. Wever, H., "Überführungsversuche an Festem Kupfer," Zeitschrift für Elektrochemie, 60, 1170-75 (1956).

20. Seith, W. and Wever, H., "Über Einen Neven Effekt bei der Elektrolytischen Überfuhrung in Festen Legierungen," Zeitschrift für Elektrochemie, 57, 891 (1953).

21. Saller, H. A., "Beneficial Effects of Radiation in Metals," Nucleonics 14, No. 9, 86 (1956).